The Thesis committee for Donald William Millsap certifies that this is the approved version of the following thesis:

Evaluation of Nylon 6,6 in Use in Fire Foe™ Fire Suppression Systems within Plutonium Gloveboxes

Approved by

Supervising Committee:

Supervisor: _____

Sheldon Landsberger

_____

Steven Biegalski

Evaluation of Nylon 6,6 in Use in Fire Foe™ Fire Suppression Systems within Plutonium Gloveboxes

By

Donald William Millsap, B.S.

Thesis

Presented to the Faculty of the Graduate School of

The University of Texas at Austin

in Partial Fulfillment

of the Requirements

for the Degree of

Master of Science in Engineering

The University of Texas at Austin

December 2012

Dedication

I dedicate this work to my mother, to whose wits I've thankfully never found the proper end, despite my thorough searching. To my father, whom I've learned the proper end of all true honesty and acceptable limits of guile. To my mother's mother, who always has good argument in store. To my father's mother, who gave me my lighter to spark good ideas. Finally, to my grandfathers, whom I owe considerable amounts of my character.

Acknowledgements

I would like to thank my advisor, Dr. Sheldon Landsberger, for his support and advice through this project. Dr. Landsberger has always offered terrific supervision throughout my graduate education and is always full of advice whenever it was needed. I would also like to acknowledge the fine folks at Los Alamos National Laboratory including Michael Cournoyer, R. T. Perry, Joe Tesmer, and Yongqiang Wang for providing the necessary guidance to make this project a success. Also, I'd like to thank the staff at the University of Texas at Austin Nuclear Engineering Teaching Laboratory for all their help in completing this project.

Abstract

Evaluation of Nylon 6,6 in Use in Fire Foe™ Fire Suppression Systems within Plutonium Gloveboxes

Donald William Millsap, MSE

The University of Texas at Austin, 2012

Supervisor: Sheldon Landsberger

Gloveboxes, where special nuclear material is handled and such as those present at Los Alamos National Labs, LANL, provide an experimental area confined within a protective shell and with strict environmental controls. These gloveboxes allow workers to indirectly interact with hazardous material. Unfortunately, these gloveboxes are not fail proof and are subject to occasional accidental failures resulting in possible breaches of containment and release of nuclear material. In particular, fires within the gloveboxes are of major concern with regard to the potential for breaches and damage to not only the glovebox but also to surrounding areas as well. Another, potentially even catastrophic, result of

glovebox fires is the potential for the spread of radioactive contamination. There is some historical precedent of contaminant release resulting from glovebox fires, such as those at the Rocky Flats Plant (Buffer, 2012).

Gloveboxes at LANL are currently equipped with manually activated fire suppression systems. In the event of an incident, a worker would hit a nearby emergency button and the system would be activated. However, this method relies on the worker to have the presence of mind in the face of danger to activate the system, and as such there is no true guarantee that the systems will be triggered. Since the level of consequence is dire, then the ideal situation requires that other fire suppression systems be present which do not rely on human interaction to function. The Fire Foe™ system has been chosen as a secondary failsafe measure in order to meet this need.

Analysis of how the casing of the Fire Foe™ system, composed of nylon 6,6 polymer, weathers under irradiation in gloveboxes is paramount in determining the effectiveness and potential lifetimes of the systems within the gloveboxes. Samples of nylon 6,6 were exposed to a 5 Ci PuBe neutron source located at the University of Texas as well as a high dose rate beam of 4.5 MeV alpha particles located at Los Alamos to determine the effect of neutron and alpha particle damage on the polymer material. Subsequent mechanical testing was conducted to determine alteration to the tensile properties of the nylon 6,6 material for both irradiated and non-irradiated samples.

The mechanical testing of the alpha ion irradiated samples suggest that most of the material damage occurs at the initial introduction of dose to a sample and is not drastically compounded with the addition of higher levels of dose. The tensile strength of the nylon after alpha particle irradiation was observed to decrease by less than 10% and the percent elongation property was not noted to vary to a statistically significant degree. The mechanical testing of the neutron irradiated samples suggests that neutrons degrade the nylon material more substantially than alpha particles. The tensile strength at both yield and break was measured to vary by nearly 20% and 10%, respectively, under neutron irradiation. The tangent modulus and the elongation at break were noted to degrade by more than 50% relative to the non-irradiated sample set.

Table of Contents

LIST OF TABLES ..... **xi**
LIST OF FIGURES ..... **xii**
CHAPTER 1: INTRODUCTION **1**
1.1 INTRODUCTION 1
1.2 GLOVEBOXES 2
1.2.1 Los Alamos Experiments 3
1.2.2 Environmental Factors 5
1.2.3 Special Concerns with Nuclear Material 7
1.3 FIRE FOE™ FIRE SUPPRESSION SYSTEM 8
1.4 OBJECTIVES OF RESEARCH 10
CHAPTER 2: NYLON AND POLYMERS UNDER IRRADIATION **12**
2.1 POLYMERS 12
2.1.1 Properties of Nylon 6,6 17
2.2 RADIATION AND DAMAGE 21
2.2.1 Alpha Particle Radiation 26
2.2.2 Neutron Radiation 30
2.2.3 Gamma Ray Radiation 34
2.2.4 Proton and Beta Radiation 35
CHAPTER 3: EXPERIMENTAL FACILITIES AND METHODS **37**
3.1 ALPHA ION BEAM TESTING 37
3.1.1 Computational Determination of Dose 38
3.1.1.1 SOURCES 4C Code *38*
3.1.1.2 MCNPX and Dose Calculation *41*
3.1.2 Selection of Alpha Particle Irradiation Source 42
3.1.3 Tandem Ion Accelerator 44
3.2 NEUTRON IRRADIATION EXPERIMENT 50
3.2.1 Neutron Irradiation Apparatus 52
3.2.2 Gold Foil Analysis 55
3.2.2.1 Gamma Ray Detection *58*
3.3 MECHANICAL TENSILE TESTING 61
CHAPTER 4: EXPERIMENTAL RESULTS **66**
4.1 ALPHA PARTICLE DAMAGE STUDIES 66
4.1.1 Color Indications of Alpha Irradiation 73
4.2 NEUTRON DAMAGE STUDIES 75
4.2.1 Neutron Specimen Discoloration 77
CHAPTER 5: DISCUSSION OF RESULTS **79**
5.1 ALPHA PARTICLE DAMAGE STUDIES 79
5.2 NEUTRON DAMAGE STUDIES 83
5.3 FUTURE AREAS OF FOCUS 85

CHAPTER 6: CONCLUSIONS.....87
APPENDIX A : ALPHA PARTICLE SOURCE DATA 90
APPENDIX B : FULL TENSILE TESTING DATA.....91
APPENDIX C : ANOVA (SINGLE FACTOR) STATISTICS OF TENSILE DATA.....94
REFERENCES.....100
VITA…….....103

List of Tables

Table 3.1 – Specifications of the PuBe Neutron Source 51
Table 3.2 – Source Strength from Gold Foils 60
Table 3.3 – Type IV Sample Specifications.....64
Table 4.1 – Alpha Particle Irradiation Results 67
Table 4.2 – Standard Deviations in Alpha Particle Results 67
Table 4.3 – Alpha Particle Results in MPa 67
Table 4.4 – Standard Deviations of Alpha Particle Results in MPa 68
Table 4.5 – Neutron Irradiation Experiment Results 75
Table A.1 – Alpha Particle Source Data 90
Table B.1 – Non-Irradiated Tensile Data.....91
Table B.2 – 1 Month Alpha Dose Equivalent Tensile Data.....91
Table B.3 – 6 Month Alpha Dose Equivalent Tensile Data.....92
Table B.4 – 1 Year Alpha Dose Equivalent Tensile Data.....92
Table B.5 – 3 Year Alpha Dose Equivalent Tensile Data.....92
Table B.6 – 6 Year Alpha Dose Equivalent Tensile Data.....93
Table B.7 – Neutron Experiment Tensile Data.....93
Table C.1 – Yield Strength No Dose/1 Month Alpha Analysis.....94
Table C.2 – Yield Strength 1 Month Alpha/6 Month Alpha Analysis 94
Table C.3 – Yield Strength 1 Year Alpha/6 Year Alpha Analysis 95
Table C.4 – Yield Strength No Dose/Neutron Dose Analysis.....95
Table C.5 – Break Strength No Dose/1 Month Alpha Analysis 95
Table C.6 – Break Strength No Dose/Neutron Dose Analysis 96
Table C.7 – Break Strength 6 Month/3 Year Alpha Analysis 96
Table C.8 – Yield Elongation No Dose/1 Month Alpha Analysis.....96
Table C.9 – Yield Elongation 3 Year Alpha/6 Year Alpha Analysis 97
Table C.10 – Yield Elongation No Dose/Neutron Dose Alpha Analysis 97
Table C.11 – Break Elongation No Dose/1 Year Alpha Analysis 97
Table C.12 – Break Elongation 1 Year Alpha/3 Year Alpha Analysis.....98
Table C.13 – Break Elongation No Dose/Neutron Dose Analysis 98
Table C.14 – Tangent Modulus No Dose/1 Year Alpha Analysis.....98
Table C.15 – Tangent Modulus 6 Month Alpha/6 Year Alpha Analysis 99
Table C.16 – Tangent Modulus No Dose/Neutron Dose Analysis.....99

List of Figures

Figure 1.1 – Typical Glovebox Setup 3
Figure 1.2 – A Golf Ball Sized Sphere of Plutonium Metal 6
Figure 1.3 – Fire Foe™ Fire Suppression System 10
Figure 2.1 – Monomer Unit of Hypalon® 12
Figure 2.2 – Segment Geometries of Polymers 13
Figure 2.3 – Phase Transition Diagram of Crystalline Thermoplastics 19
Figure 2.4 – Cross-linking Process of Irradiation 24
Figure 2.5 – Scission Process of Polymer Irradiation 24
Figure 2.6 – Grafting Processes, Three Modes 25
Figure 2.7 – Curing Process of Polymeric Irradiation 25
Figure 2.8 – Specific Ionization of an α-Particle in Air 28
Figure 3.1 – SOURCES 4C Two-Region Problem 40
Figure 3.2 – Tandem Ion Accelerator 45
Figure 3.3 – Primary Alpha Particle Beam Line 46
Figure 3.4 – Exterior of the Sample Chamber 46
Figure 3.5 – Interior of the Sample Chamber 47
Figure 3.6 – Close-up of the Interior of the Sample Chamber 47
Figure 3.7 – Nylon 6,6 Samples Loaded on Target 48
Figure 3.8 – Sample Loading 49
Figure 3.9 – Samples in Beam 49
Figure 3.10 – PuBe Neutron Source Spectrum 52
Figure 3.11 – Sample Holder with Samples 53
Figure 3.12 – Sample Holder with Container 54
Figure 3.13 – Modified Neutron Apparatus 55
Figure 3.14 – Neutron Absorption Cross Section vs. Neutron Energy for ^{113}Cd 58
Figure 3.15 – Efficiency of the HPGe Detector 60
Figure 3.16 – Typical Material Stress-Strain Curve 62
Figure 3.17 – Nylon 6,6 Tensile Samples 63
Figure 3.18 – Type IV Tensile Sample Specifications 64
Figure 3.19 – Instron Testing Machine 65
Figure 4.1 – Tensile Strength at Yield vs. Alpha Particle Dose 68
Figure 4.2 – Tensile Strength at Break vs. Alpha Particle Dose 69
Figure 4.3 – Percent Elongation at Yield vs. Alpha Particle Dose 70
Figure 4.4 – Percent Elongation at Break vs. Alpha Particle Dose 71
Figure 4.5 – Tangent Modulus vs. Alpha Particle Dose 72
Figure 4.6 – Discoloration of Nylon 6,6 after Alpha Irradiation 73
Figure 4.7 – Nylon 6,6 Sample Cross Sections after Alpha Irradiation 74
Figure 4.8 – Discoloration of Nylon 6,6 after Neutron Irradiation 77

Evaluation of Nylon 6,6 in Use in Fire Foe™ Fire Suppression Systems within Plutonium Gloveboxes

Chapter 1: Introduction

1.1 INTRODUCTION

Los Alamos National Labs, LANL, is a key center of nuclear and scientific research within the United States. A significant portion of that research relies on the use of gloveboxes for the containment of nuclear and otherwise hazardous experiments. These gloveboxes serve as a primary engineering control for the isolation of dangerous material. These boxes are typically designed so that large experiments can be run within and handled by multiple workers at various glove access ports. This being the case, one of the paramount concerns at Los Alamos is maintaining these gloveboxes so that they are able to operate safely without risk of a serious incident occurring. Failure of a glovebox would likely involve the release of radioactive material, resulting in probable exposure to workers and the indoor and possible outdoor environments. Such an event would lead almost certainly to facility and laboratory closure, worker downtime and extensive decontamination and cleaning of facilities. The consequences would also likely be very costly both monetarily and politically. (Griffen, 2006)

Previous studies conducted by the University of Texas in conjunction with Los Alamos have examined weaknesses in the gloveboxes from ruptures and tears in the materials composing gloves (Casey, 2004 and Griffen, 2006). However,

another chief concern with the experiments conducted within the gloveboxes is the possibility of a catastrophic fire. There exists an inherent risk of fire in some of the materials used in glovebox experiments. As a means of reducing the potential for fires to propagate in gloveboxes, a new fire suppression system has been added to existing gloveboxes. The selected fire suppression system is the Fire Foe™ system which automatically deploys in case of a fire without the need for human intervention. This paper shall begin by providing an introduction into the glovebox experimental environment and move forward into a discussion of the behavior of the nylon 6,6 polymer casing of the fire suppression system under irradiation.

1.2 GLOVEBOXES

As stated, gloveboxes are primarily used in cases where experimentation or other processes would be much too hazardous in an open environment. Gloveboxes also allow for tailored environments within the box such as altering pressure, temperature, and other atmospheric qualities. It is the principal purpose of a glovebox to serve as an isolation unit to contain materials undergoing work or research. The focus of this research is limited to those gloveboxes in use at the Los Alamos nuclear facilities. A typical glovebox apparatus can be seen in Figure 1.1 below, and consists of a support structure, steel outer casing, view ports for workers with leaded glass, polymer gloves, ventilation, and internal shielding composed of leaded material.

Figure 1.1: Typical Glovebox Setup. Pictured is a standard glovebox with several glove ports closed and sealed as well as several gloves ready for use with experiments within the gloveboxes (Cournoyer, 2008).

1.2.1 Los Alamos Experiments

The gloveboxes in current usage at the Los Alamos National Laboratory Plutonium Facility under the operation of the Nuclear Materials Technology division, or NMT, are utilized to perform a wide array of experiments. The various groups within the NMT division are responsible for the following operations using gloveboxes (Cournoyer, *et al.*, 2004):

- ***Actinide Process Chemistry*** – Provide aqueous recovery operations; pyrochemical operations converting oxides to metal; further purification, research, and activities to advance basic scientific knowledge.

- ***Weapons Component Technology*** – Provide pit surveillance, fabrication, assembly, and engineering services for the stewardship of plutonium components in the nation's nuclear weapon stockpile.
- ***Plutonium-238 Science and Engineering*** – Handle significant quantities of ^{238}Pu oxide, metal, and solution in un-encapsulated forms.
- ***Actinide and Fuel Cycle Technologies*** – Work toward the stabilization and storage of plutonium oxide materials, and the development of transmutation fuel forms.
- ***Pit Disposition Science and Technology*** – Dismantle pits of nuclear weapons, convert plutonium from pits into oxides, and perform nuclear fuel activities.
- ***Nuclear Materials Science*** – Characterize new and aged pit construction materials and develop technologies to characterize actinide materials.
- ***Actinide Analytical Chemistry*** – Focus on the analysis of samples in actinide matrices; determining the assay and isotopic composition of actinide metals and oxides, and trace impurities in samples.

Depending on the particular purpose and nature of the experiments within a given glovebox, the internal environmental conditions can vary considerably from box to box. These environmental conditions tend to act detrimentally to any metallic or polymeric materials present within the gloveboxes. The polymeric materials, specifically, are important in the design of both the gloves within gloveboxes as well as the fire suppression materials used within gloveboxes.

1.2.2 Environmental Factors

The particular environmental conditions which are of concern with respect to polymer degradation within gloveboxes include irradiation from nuclear sources, chemical corrosion from strong acids used in some boxes, and also atmospheric conditions such as excessive heat from thermal sources and apparatuses used for glovebox experiments. The radiological hazards introduce radiation to the materials within the glovebox in the form of alpha and beta particles, as well as neutrons, particularly fast neutrons, and gamma rays. (Griffen, 2006) These sources are also not necessarily confined to solid geometric bodies, such as metallic spheres an example of which is shown in Figure 1.2, but rather they may also exist in a metallic-oxide particulate state, or a sort of radioactive dust, within the gloveboxes (Casey, 2004).

These particulate forms are more an issue with regards to alpha irradiation damage in materials. This is due the ability of the dust to coat the inner surfaces of a glovebox and cake into relatively thick layers. In some of the highest dose plutonium gloveboxes, the boxes are filled with alpha particles released from plutonium oxide particulates to the point that the density of the metallic-oxide causes the inside of the box to become completely obscured to external viewers. Alpha particles normally have a very short distance of travel before they are absorbed into media, meaning they have a very high linear energy transfer, or LET (Was, 2007). Thus if an alpha emitting nuclear source in the form of dust is in close contact with other material within a glovebox, then it should tend to result

in a higher degree of dose in the material from these particles. The effect of this dose on nylon 6,6 polymer specimens is one part of the subject of this study.

The primary alpha particle emitters present in a glovebox at LANL include the isotopes ^{238}Pu and ^{239}Pu within plutonium oxide molecules (Casey, 2004). ^{238}Pu emits alpha particles through its primary mode of decay to ^{234}U with a half-life of 87.7 years with energy of 5.593 MeV. ^{239}Pu emits alpha particles through decay to ^{235}U with a half-life of 24,110 years with emitted energies of 5.106, 5.144, and 5.157 MeV. Neutrons are generated from secondary (α, n) reactions within the plutonium oxide as well as through direct emissions from decay. In the case of the (α, n) reactions, the alpha particles emitted by the Pu isotopes have a chance of causing a reaction with the isotopes of oxygen and emitting a neutron as a result. (KAERI, 2000)

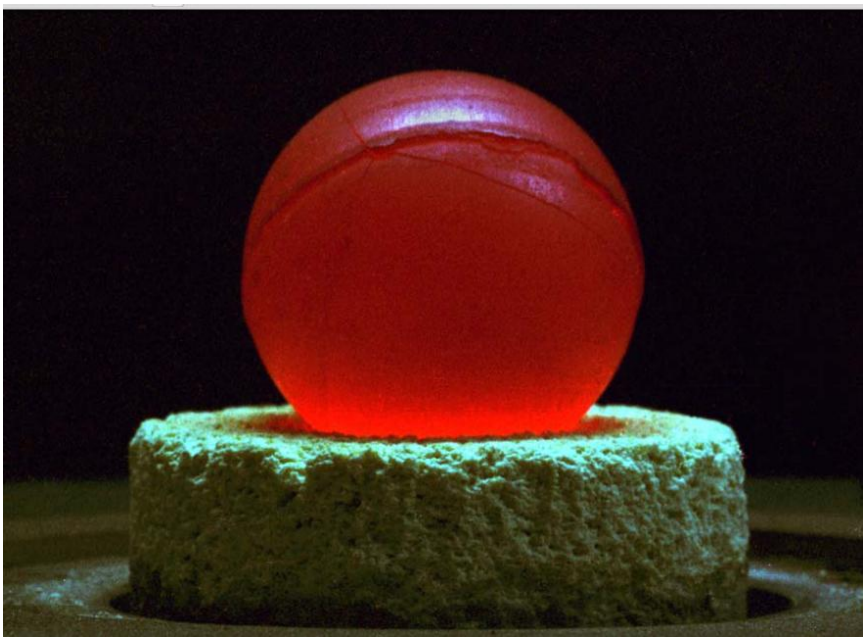

Figure 1.2: A Golf Ball Sized Sphere of Plutonium Metal. The Pu sphere not only puts out significant radiation, but also emits enough heat to glow visibly red hot (Cournoyer, 2006).

1.2.3 Special Concerns with Nuclear Material

There is a special danger presented from nuclear sources such as pure uranium and plutonium metals in addition to their natural radioactivity. These substances have a special classification and are known as pyrophoric materials, and as such pose a significant fire risk. By definition, a pyrophoric material is one which is capable of spontaneous combustion when placed in an oxygen enriched environment (Plutonium Properties, 2005). Typically, when plutonium metal combusts it does not erupt into flames immediately, but rather the material smolders in a way similar to how charcoal burns (Plutonium Properties, 2005; Buffer, 2012). Historically, this property of plutonium has been responsible for a number of glovebox fires, ranging from small to catastrophic, at facilities which house plutonium gloveboxes, including the now defunct Rocky Flats nuclear weapons production facility outside of Denver, Colorado (Buffer, 2012).

Notable plutonium glovebox fires include fires at the Rocky Flats facility occurring in 1957 and again in 1969. The 1957 glovebox fire began when a plutonium metal source underwent spontaneous combustion due to interaction with air within the glovebox. The fire quickly spread through the laboratory building in which the glovebox was housed. The fire ultimately involved an estimated 13 to 21 kg of plutonium material leading to an estimated release of 300 grams or nearly 20 Ci of radioactive material to the environment. At least some of the radioactive material released from this event was determined to have reached the greater Denver metropolitan area. (Buffer, 2012)

The 1969 Rocky Flats fire began in a similar fashion to the 1959 fire, however due to increased safeguards placed on the laboratory's ventilation system the damage caused by this fire was greatly reduced. There was an estimated release of 0.2 to 1 gram of radioactive material from this fire. (Buffer, 2012) Following the construction of the current plutonium facility at Los Alamos in the 1970s, the lessons learned from these two blazes were incorporated into glovebox designs (Leonard, 1999).

The glass used in early plutonium gloveboxes was crafted from Benelex and Plexiglas. This material was a primary reason for the spread of glovebox fires because of their combustible nature. This concern has been mitigated greatly by constructing gloveboxes with non-combustible glass and lined with stainless steel. However, fires originating within a single glovebox can still propagate under certain conditions. If there is a sufficient amount of hot, combustible gases present that are then able to be transported through ventilation ducts to other gloveboxes within a facility or to other areas within the facility containing combustible materials, then it becomes possible for fires to propagate beyond the initial glovebox. For this reason, it becomes imperative to extinguish glovebox fires quickly and within the confines of the originating glovebox before they are allowed to spread. (Leonard, 1999)

1.3 FIRE FOE™ FIRE SUPPRESSION SYSTEM

Given the predisposition of plutonium to catch fire, the adequate placement of fire suppression systems within gloveboxes is important to ensure

the continual, safe operation of these gloveboxes. Systems currently in use rely on standard fire suppression methods with the fire quenching material being supplied via external piping. This system is activated at certain strategic points within the lab environment by human workers in the case of an emergency. However, human workers are subject to the effects of natural instincts, such as panic, and as such their reliably to activate the systems is not absolute. There also exists the possibility of workers becoming injured or else impaired in attempting to activate these systems due to the nature of a particular emergency. For this reason, a supplemental system is needed that does not rely on being triggered by workers in order to function properly. The new system that has been chosen to fit this role is the Fire Foe™ fire suppression system supplied by Quick Fire.

The Fire Foe™ fire suppression system, shown in Figure 1.3 below, is composed of a nylon 6,6 tube casing containing a sodium bicarbonate powder filling and a inert gas, hexafloroupropane. In the event of rupture of the tube casing as would happen in the event of a fire, the powder explodes outward covering an enclosed area up to 3.7 m^3 and immediately extinguishing a fire. The powder is kept at a fully charged pressure of 100 psi, or 689.5 kPa, within the tube casing. The tubes are designed to be completely stable below 80 °C and to instantaneously discharge at temperatures above 150 °C. However, the tubes are capable of reacting to slow building fires in addition to flash fires. The tubes are also designed to be resistant to corrosion and abrasive wear. These qualities make them appropriate for use in gloveboxes. (Quick Fire, 2011)

Figure 1.3: Fire Foe™ Fire Suppression System. This system is entirely self contained and requires only to be affixed to a surface in the area needing fire protection. (Quick Fire, 2011)

1.4 OBJECTIVES OF RESEARCH

The Fire Foe™ system utilizes a number of different materials in its construction that are each subject to the effects of irradiation. In particular, the casing of the system is composed of form set nylon 6,6. This material is very common and has been studied under an array of different radiation types and dose levels (Deely, 1957; Ellison *et al.*, 1984; Fadel *et al.*, 1989; Olivares *et al.*, 1996; and Chen, 2011). However, this material has not been well studied under high dose alpha particle irradiation conditions such as what is likely in very high dose plutonium gloveboxes at LANL. Therefore, this research aims to age nylon 6,6 samples artificially under conditions similar to that of a glovebox. Specifically, the goals set forth are:

- irradiating samples of the fire suppression system's nylon 6,6 casing material using an alpha particle ion beam to simulate conditions in a worst case glovebox,

- irradiating the nylon 6,6 material using a PuBe neutron source,
- examining material properties of the casing both before and after irradiation through the use of mechanical tensile testing techniques, and
- determining the viability of the Fire Foe™ system placed within the glovebox environment over a projected length of time.

Chapter 2: Nylon and Polymers under Irradiation

2.1 POLYMERS

Polymers are complex molecules formed from the interlinking of several simpler molecules. These simpler compositional molecules are sometimes referred to as monomers, and hence several of them linked become a polymer. A typical example of a monomer unit is shown in Figure 2.1. The structural units of the polymer are usually bound together through covalent chemical bonding. The term polymer is often synonymous with plastics; however, the category of polymers is much broader in scope than only plastics. In addition to artificial polymers such as plastics and elastomers like nylon, polymers that occur in nature include biopolymers such as proteins and DNA molecules which are the basic building blocks of all life. Polymers also include natural materials such as amber and natural rubber, which have been used by humans for centuries. (Corneliussen, 2002, DOE Handbook, 1993)

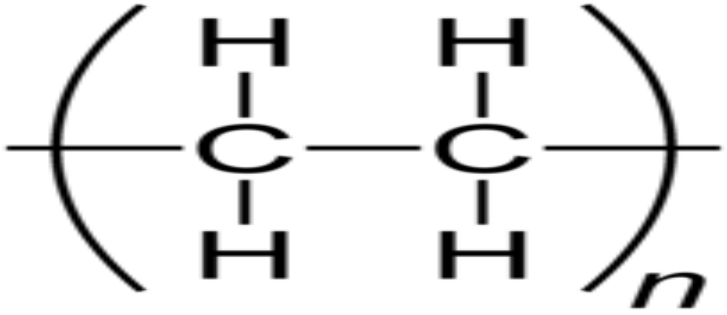

Figure 2.1: Monomer Unit of Hypalon®. This is a singular molecular component of the polymer material Hypalon produced by DuPont. In the full polymer chain, there would be *n* units of this monomer linked through covalent electronic bonds. (Hypalon, 2005)

Most organic polymers are composed of monomer units primarily containing simple hydrocarbons, or molecules of carbon atoms bonded to hydrogen atoms such as CH_3. Polymeric molecules are often linked to one another with interstitial atoms such as nitrogen to facilitate the growth of very long molecular chains. These chains are able to twist and fold over one another and are bound together through bonds along the side groups within the chain. Polymers can be formed such that this twisting and folding creates layered and ordered structures. These ordered structures are referred to being crystalline polymers. The reverse of this are the group of polymers known as amorphous polymers. Amorphous polymers do not take an ordered structure and take a more random orientation to layering of the chains. Polymer matrices are capable of being regionally amorphous or crystalline, as shown in Figure 2.2, and can be classified by their percentage of total crystallization. (DOE Fundamentals Handbook, 1993)

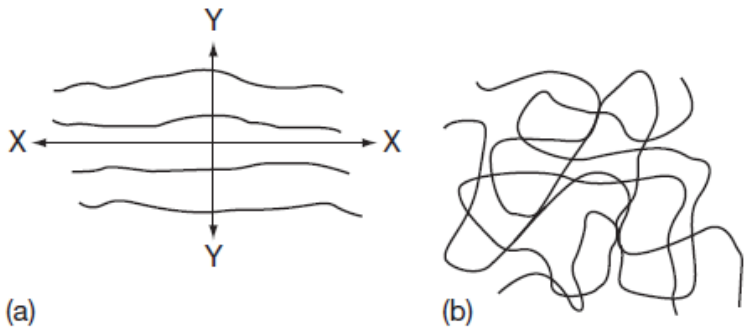

Figure 2.2: Segment Geometries of Polymers. Crystalline polymers, a), have regions of highly ordered layering of the polymer chains. Amorphous polymers, b), have regions with higher degrees of randomness to the orientation of polymer molecules in the chain. (Hourston, 2010)

Polymers are formed through the chemical process known as polymerization. There are several different modes by which a polymer may be constructed through polymerization including free radical addition of monomers, step-growth polymerization, rearrangement, and ionic polymerization. In the case of free radical addition of monomers, the double bond present in a simple molecule such as ethylene allows for that molecule to become bonded with other similar molecules as shown below:

$$nCH_2 = CH_2 \rightarrow [-CH_2 - CH_2 -]_n, \quad \textbf{(2.1)}$$

where n is the number of monomer units in the final polymer chain which typically ranges from 10,000 to over 1,000,000 units. In step-growth polymerization, there is a chemical reaction between two molecular groups that leads to the production of both a polymer and a small molecule such as water. This method is used in the production of the polymer as shown below:

$$nHOOC(CH_2)_4COOH + nH_2N(CH_2)_6NH_2 \rightarrow$$
$$[-OC(CH_2)_4CONH(CH_2)_6NH -]_n + 2nH_2O, \quad \textbf{(2.2)}$$

where the two reactants are adipic acid and hexamethylene diamine. A great number of plastics are produced in this method, including most nylons and polyesters. (Hourston, 2010)

Rearrangement polymerization is similar to the step-growth process, with the exception that no smaller molecule is produced as a result of the forming chemical reaction. For example, the molecule of polyurethane is produced as follows:

$$nHO(CH_2)_4OH + nOCN(CH_2)_6NCO \rightarrow$$
$$[-O(CH_2)_4OOCNH(CH_2)_6NHCO-]_{n,} \quad \textbf{(2.3)}$$

where the reactants are 1,4 butane diol and hexamethylene di-isocyanate. This method is also used to produce nylon 6 from the ring compound ε-caprolactum. Finally, in the case of ionic polymerization, the growth of polymer chains is stunted or terminated using ionic groups. The key advantage of this type of polymerization is that it allows a high degree of control in the final form of the molecular chain architecture. Polymers can also be readily obtained from natural biological sources such as cellulose taken from wood or cotton as well as chitin taken from the shells of crustaceans. (Hourston, 2010)

Polymers have a wide arrangement of uses in industry, commercial, medical, and academic research fields. Plastic polymers are polymers of high molecular weight that at some point in their formation achieve a fluidic flow. However, plastics are often brought to a more solid and rigid form for end user applications. The category of plastic polymers is differentiated from the general term ‘plastic’ which is used to describe a type of deformation behavior of polymers under applied stress. Plastic deformation occurs when polymers that

remain relatively rigid under no applied stress or strain then deform greatly under applied stress and do not recover their initial properties, such as when a spring is pulled too far and remains elongated. Plastics are often used for hard casing of low temperature electronics, storage units, and various other applications. (Hourston, 2010)

Elastomers, or polymers that exhibit at least some degree of elastic behavior, will rebound back to their original shape after being subjected to an applied stress below a certain level. Beyond the elastic limit, additional applied stress results in plastic deformation of the material. These elastomers are used often in cabling and insulation of electrical wiring, in situations of high external stress as in tires for an automobile, and in some polymer based laboratory glassware. Other common uses of polymers include artificial sponges, clothing, vacuum seals, and various other commonplace household items that are encountered on a daily basis. The wide usage of polymers illustrates the point that they are among the most versatile materials available for use in the modern world. (Hourston, 2010)

Polymers also see an extensive use in nuclear environments. Hypalon® and polyurethane, in particular, are used extensively as materials for gloves in gloveboxes. These materials have been studied extensively under accelerated aging conditions including corrosion and irradiation (Casey, 2004, Griffen, 2006). Nylon 6,6 is another material used within the glovebox environment and is the principal component of the casing of the Fire Foe™ system. Therefore, it is

important to understand how nylon 6,6 ages under conditions within a plutonium glovebox at Los Alamos.

2.1.1 Properties of Nylon 6,6

Nylon 6,6 is a member of a group of plastic materials that are referred to, collectively, as nylon. Nylon is one of the most common synthetic polymers available today. It was developed by the DuPont Company's Wallace Carothers in 1935 to serve as an artificial alternative to silk for clothing, fibers and other industrial applications. Following the Second World War, nylon saw extensive use in carpeting, ropes, and other applications where natural fibers such as cotton and silk were in reduced supply. Nylon 6 and nylon 6,6 are the most common variations of nylon and consist of monomer units with 6 carbon atoms, several hydrogen atoms, and interconnected by either oxygen or nitrogen atoms. The formulation of nylon 6,6 from adipic acid and hexamethylene diamine using step-growth type polymerization was previously described and given in equation 2.2. (Trossarelli, 2010)

Nylon 6,6 is a type of polymer also known as a thermoplastic polymer. A major benefit to using thermoplastic polymers is that they can be softened or partially melted through heating and then reformed into a desired casted mold or shape while retaining their properties. There are four distinct types of thermoplastic polymers: amorphous, rubber-modified amorphous, plasticized amorphous, and crystalline thermoplastics. Amorphous thermoplastics are composed of polymers that have a sufficient degree of irregularity in their

molecular structure to prohibit crystallization. At low temperature, amorphous thermoplastics are rigid and glass-like and at sufficiently high temperatures the material becomes softened and can take on rubberized qualities. The temperature at which this occurs is known as the glass transition temperature of the polymer. Rubber-modified thermoplastics are amorphous thermoplastics that have been strengthened with the addition of rubbery polymers dispersed through the larger polymer matrix. Plasticized thermoplastics are plastics that have been mixed with certain high boiling temperature, low level volatility liquids in order to reduce the temperature at which these plastics are able to transition from a rigid state to a softer, more rubber-like state. (Hourston, 2010)

Crystalline thermoplastics are the final group of thermoplastics and the category to which nylon 6,6 belongs. These polymers do not show the usual external signs of crystallization, such as macroscopic geometric formations. However, these polymers do exhibit several properties common in crystalline materials. Specifically, these polymers show distinct X-ray diffraction patterns as well as specific melting in differential scanning calorimetry. It is important to note that the entirety of such polymer matrices may not be in a crystalline structure, but rather segments or portions of the polymer will pass through hot spots where the molecules follow a highly ordered arrangement. The hot zones serve as a means of cross-linking the individual molecules of the polymer together and strengthening the overall polymer matrix. (Hourston, 2010)

The effect of temperature on crystalline thermoplastics is more complicated than for the other three forms of thermoplastics. A typical crystalline

thermoplastic polymer will begin with a structure that is hard and rigid at lower temperatures. As a polymer is raised through its glass transition temperature, the material will soften to a leather-like quality, but only for polymers that have a lighter degree of crystallinity. For polymers that are highly crystallized, there is much less softening and change at the transition temperature. The polymeric crystals will then proceed to melt upon further addition of heat to the material, and the polymer will become soft and rubbery. The range of temperatures required to completely transition a polymer from crystalline to soft and rubbery vary over a wide range and are dependent on the particular polymer in question as well as its molecular weight. (Hourston, 2010)

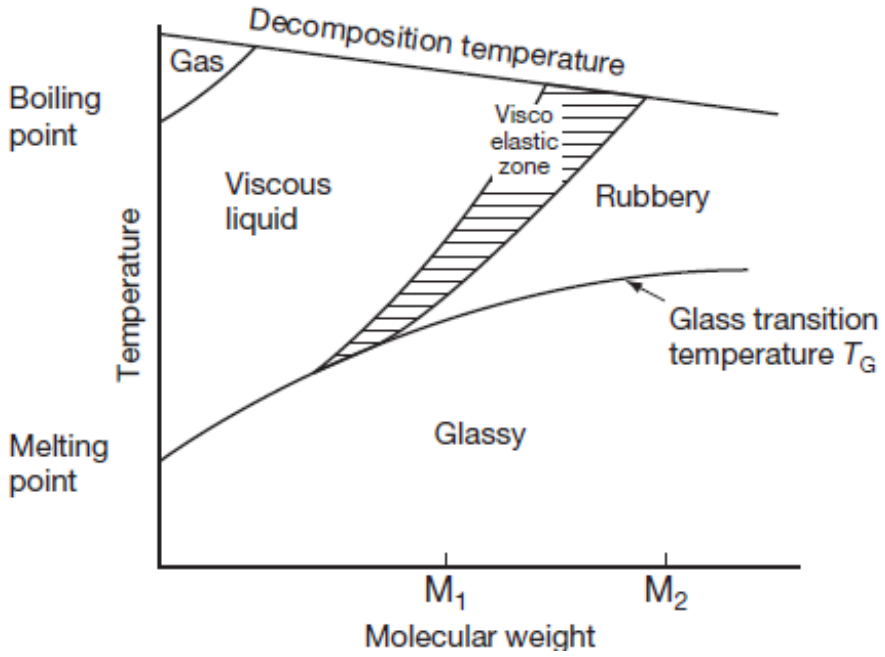

Figure 2.3: Phase Transition Diagram of Crystalline Thermoplastics. Crystalline polymers with a higher molecular weight will transition to a rubbery state at higher temperatures (Hourston, 2010).

In general for crystalline thermoplastics, the tensile strength of the polymers is typically at least as high as amorphous thermoplastics for temperatures under the glass transition temperature. Between the melting point and glass transition temperature of a thermoplastic polymer, the tensile strength and rigidity of the polymer becomes highly dependent on the level of crystallinity and molecular weight of the polymer. Also, crystalline thermoplastics tend to be opaque to the transmission of light. This is due to difference in densities between the crystalline and more amorphous areas within the polymer matrix. At the boundaries between the crystalline and amorphous zones, there is a surface at which light will readily scatter. (Hourston, 2010)

Nylon 6,6 takes on all the general qualities of a crystalline thermoplastic. However, the physical properties of the polymer are highly varying and depend strictly on the degree of crystallization within the particular matrix of a given sample of nylon. That is to say, one batch of nylon 6,6 will exhibit different properties than a similar batch with lower levels of crystallinity. Nylon 6,6 has a melting temperature of 255 to 265 °C, and an elongation at break of 15 to 80%. At the highest level of crystallization, the polymer has a density of 1.24 g cm^{-3} and at low crystallization levels the polymer has a density of 1.07 g cm^{-3} at room temperature. The tensile strength at yield ranges from 8,000 to 12,000 psi, or 55.16 MPa to 82.74 MPa, under dry conditions, and the tensile strength at break is typically near 14,000 psi, or 96.53 MPa. The tensile modulus of the polymer ranges from 230,000 to 550,000 psi, or 1.59 GPa to 3.79 GPa, under dry conditions. (Corneliussen, 2002)

2.2 RADIATION AND DAMAGE

The effect of radiation present on nylon 6,6 from sources within gloveboxes is the central focus of this research. The main source of radiation within these boxes has been previously stated to be ^{238}Pu and ^{239}Pu which primarily emit alpha particles. However, through (α, n) reactions with oxygen atoms chemically bonded to the plutonium atoms, neutrons are also produced within the gloveboxes. Neutrons and gamma rays can also be produced through decays of plutonium isotopes (Kaeri, 2000). The interaction of these particles with polymers has been studied at length and with special regard to conditions within a glovebox (Casey, 2004, Griffin, 2006). Various types of nylon, in particular, has been extensively reviewed under various types of irradiation including neutrons, gamma rays, beta particles and high energy protons. Therefore, it is prudent to give a brief overview of the different types of radiation and how they interact with nylon specifically in addition to the general characteristics of radiation damage to polymers.

The effect of radiation on materials is the subject of extensive studies. While the behavior of irradiated materials such as steel and other metals, which take on simplistic crystalline molecular structures, is well understood, polymers and other highly sophisticated molecules are the subject of ambiguity with regards to behavior under irradiation (Was, 2007). In general, polymers are weakened or destroyed through the breaking of the chemical bonds holding together the atoms within the polymer matrix. The severing of bonds occurs during irradiation primarily through the ionization of atoms within the polymer matrix or through

directly displacing those atoms from their matrix placement (Bhattacharya, 2000). Absorption of energy from radiation into the polymer matrix causes the polymer chain to become fragmented. The polymer fragments then react with the remaining base polymer matrix which leads to the creation of free radical molecules (Bhattacharya, 2000). Under higher levels of radiation dose, this effect can lead to the complete dissociation of the polymer matrix into a "soup" of molecules with low molecular weight (Chapiro, 1995).

Radiation will cause four different types of reactions within polymers: cross-linking, scission, grafting, and curing. Cross-linking is the formation of intermolecular bonds between polymer chains within a matrix. The number of cross-linked molecules increases proportionally with the dose received from radiation. However, it does not typically vary greatly with chemical structure of the irradiated polymer or the temperature at which irradiation occurs. The effect of cross-linking on a given polymer matrix is such that the polymer will grow in molecular weight and the chains within the matrix will eventually network into a 3-dimensional structure. This buildup of a 3D polymer matrix essentially strengthens the overall polymer. Scission is, fundamentally, the opposite of cross-linking. Typically, scission will occur when bonds between two conjoined carbon atoms are severed within a polymer. This leads to a lowering of the molecular weight of the polymer and eventual dissolution of the material under high levels of irradiation, i.e. the soup effect described previously. A diagram showing both the cross-linking and scission process is given in Figures 2.4 and 2.5 below. (Bhattacharya, 2000)

Grafting is a process by which monomers will be introduced and bound into a polymer matrix. In the simplest case, the base polymer matrix takes the form of a thin film, fiber, or powder with the grafted monomer taking the form of a neat liquid, solution or a vapor. During the grafting process, covalent C-C bonds are formed between the introduced monomer and the base polymer over the course of several minutes, hours, or days. Grafting can occur in three separate modes including pre-irradiation, peroxidation, and the mutual irradiation technique. In the pre-irradiation mode, the base polymer is irradiated within a vacuum or in an environment filled with an inert gas. This creates free radicals which are then able to form bonds to a monomer that is then introduced to the system. The peroxidation method uses high energy irradiation on the base polymer in the presence of oxygen in order to stimulate the growth of peroxide chemical groups. The monomer compound is then added to the system at an elevated temperature. The mutual irradiation technique requires that the monomer and polymer base be irradiated simultaneously in order for free radicals from both to facilitate new bonds. Illustrations of the various modes of the grafting process are given in Figure 2.6. The last form of radiation reaction with polymers is curing. Curing involves the rapid polymerization of a monomer mixture to a base polymer such that it forms a coating on the base bound by mostly physical forces. An example of the curing process is given in Figure 2.7 below. (Bhattacharya, 2000)

(1) Crosslinking

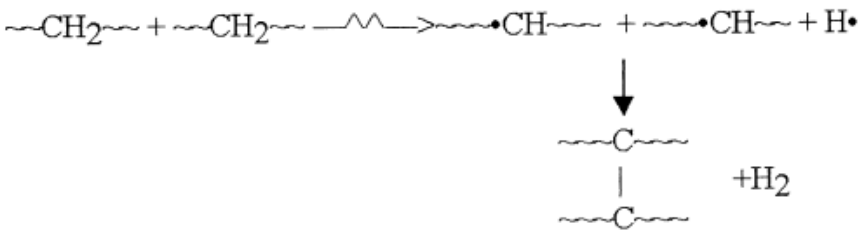

Figure 2.4: Cross-linking Process of Irradiation. A simplistic representation of the first polymer irradiation process is shown. (Bhattacharya, 2000)

(2) **Scission**

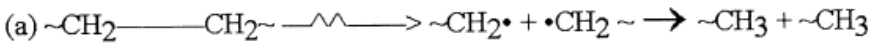

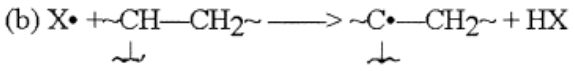

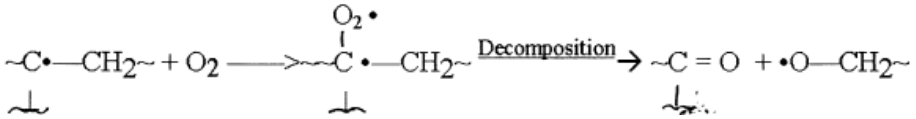

Figure 2.5: Scission Process of Polymer Irradiation. Chemical reaction of the deconstruction of a polymer by scission is shown. (Bhattacharya, 2000)

(3)(a) *Grafting* (*pre-irradiation*):

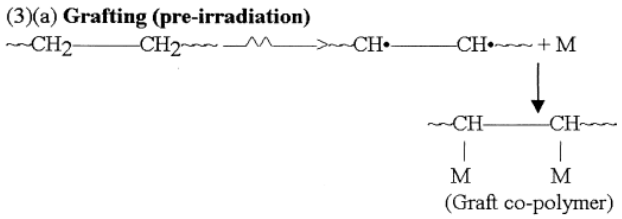

(3)(b) *Grafting* (*peroxidation*):

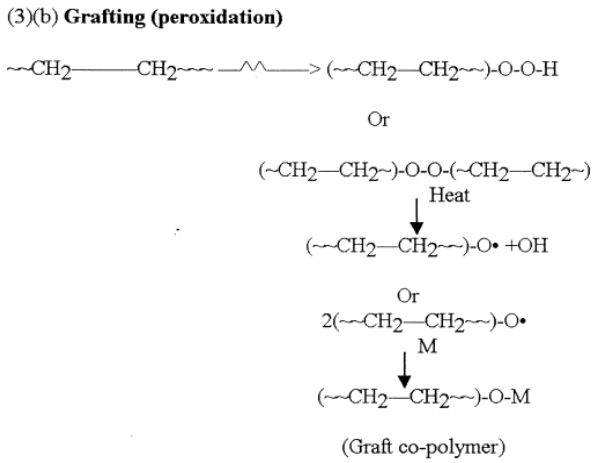

(3)(c) *Grafting* (*mutual irradiation*):

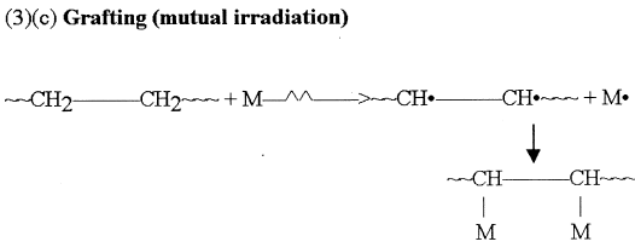

Figure 2.6: Grafting Processes, Three Modes. The above three methods require the external addition of a monomer to the polymer base during irradiation. (Bhattacharya, 2000)

(4) *Curing*:

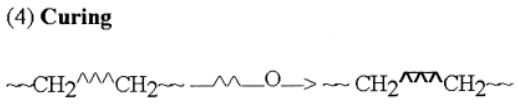

Figure 2.7: Curing Process of Polymeric Irradiation. Here is the irradiated polymer reaction type which requires the external addition of a monomer to the system and a rapid repolymerization of the matrix. (Bhattacharya, 2000)

2.2.1 Alpha Particle Radiation

An alpha particle is the ionized nucleus of a helium atom, or He^{++}, consisting of 2 protons and 2 neutrons. Alpha particles and other charged particles, such as protons and heavier ions, belong to a class of radiation known as directly ionizing radiation. Directly ionizing radiation will create a trail of excitation and ionization through the medium material that the radiative particle travels. This trail is a result of the electrical coulomb forces from the ionizing ion interacting with the electron shell of the atoms of the medium. Alpha particles and other heavy ions have a high linear energy transfer, or LET. A particle with higher LET than another particle with identical energy will deposit its energy into a traversed medium more quickly; or rather that the particle deposits more energy per unit distance within the medium. (LaMarsh, 2001)

For alpha particles in particular, most of the energy of the doubly ionized He^{++} ion is deposited into the target medium through Coulombic interactions with the electrons of the medium. The electrons gain energy and are ejected from their previous positions within the atomic and molecular structures of the medium resulting in ionization. An He^{++} ion will subsequently lose energy and slow as it passes through a material. It is also possible for alphas and charged particles to interact with the nucleus of the atoms within the medium and deposit nearly all of their energy at once, although this sort of interaction has a very low probability of occurrence. (Casey, 2004)

As a consequence of the high LET of alpha particles, the range of these particles through a medium is typically very small. For an alpha particle with

energy of 6 MeV, the range of the particle traveling through air at room temperature is less than 5 cm. Correspondingly the number of ionizations produced through the path of such an alpha particle bottoms out at approximately 5 cm as shown in Figure 2.8. The range of alphas through other materials is typically determined using the *Bragg-Kleeman rule*:

$$R = R_a \left(\frac{\rho_a}{\rho}\right) \sqrt{\frac{M}{M_a}}, \qquad \textbf{(2.4)}$$

where R is the range of the alpha of E energy through the material, ρ is the density of the material, M is the molecular weight of the material, R_a is the range of alphas of E energy through air, ρ_a is the density of air, and M_a is the average molecular weight of air at room temperature. Here the range of alpha particles in air is typically obtained from a chart based on the particle energy. (LaMarsh, 2001)

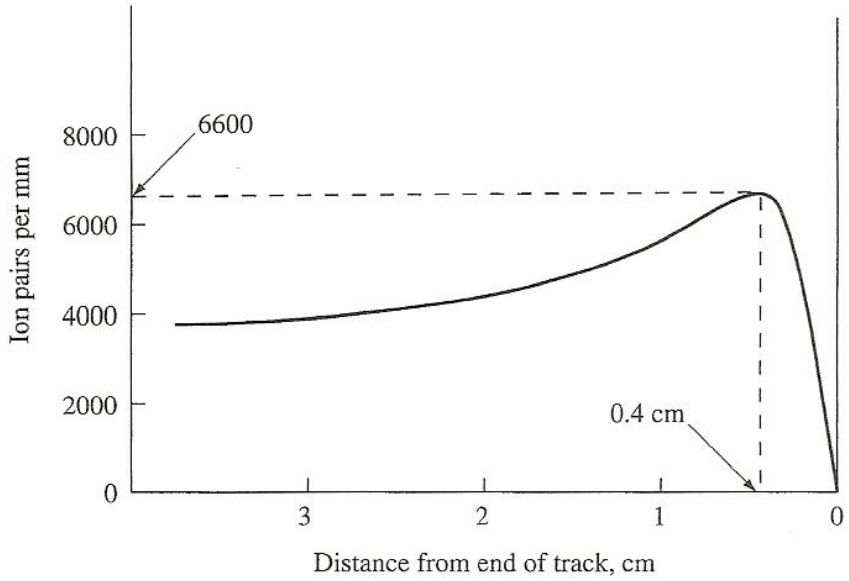

Figure 2.8: Specific Ionization of an α-Particle in Air. This plot demonstrates the number of ion pairs produced in air by an alpha particle moving through a thickness of air. (LaMarsh, 2001)

Radiation types with higher LET also have a higher quality factor or radiation weighting factor. The radiation weighting factor, W_R, is a value assigned to types of radiation energy of radiation. The radiation weighting factor is directly proportional to the amount of equivalent dose a biological system will receive from the corresponding radiation given a certain absorbed dose. This weighting factor is also somewhat useful for radiation damage to polymers and other organic molecules given their chemical similarities to biological systems. Particles with low LET such as beta and x-rays have a weighting factor value of 1, whereas alpha particles have a weighting factor of 20. Thus, for the same level of absorbed dose from both an x-ray source and alpha particle source, the alpha particles will have a much higher effective dose on a material. (LaMarsh, 2001)

Previous work involving alpha particle irradiation of polymers has included efforts to irradiate samples to high doses using alpha particle ion beams

as well as low dose irradiations using small point sources (Murphy, 2004, Griffin, 2006). However, the previous ion beam studies have focused primarily on introducing enough irradiative dose to thin polymer films to dissociate the constituent molecules into volatile elements (Murphy, 2004). This method, as previously used, did not attempt to account for the conditions within plutonium gloveboxes, however it can be very easily tailored for that application. The other method of employing a low dose point source did not yield viable results due to issues with the experiment (Griffin, 2006). Neither of these experiments were used, specifically, on the polymer nylon 6,6, and as such specific studies of how this polymer behaves under alpha particle irradiation are seemingly few and far between.

The lack of available studies may be due in part to the minute range of transmission of alpha particles through material as stated previously. Most situations where alpha particle radiation is of concern either do not have alpha particles in close enough contact with material to do damage, or else there is adequate shielding to protect materials from incident alpha particles. Also, most dose and damage concerns from alpha particles are typically focused on potential biological harm to workers resulting from contamination of alpha emitting isotopes. However, since the gloveboxes at Los Alamos are constructed such that the entire interior of particular gloveboxes can be expected to be completely coated with plutonium oxide dust in the worst case scenario, then the study of how the nylon 6,6 casing material of the Fire Foe™ system performs under close contact alpha irradiation becomes paramount.

2.2.2 Neutron Radiation

Neutrons, as their name implies, are the electrically neutral component of an atomic nucleus. Neutrons not bound to the nucleus of an atom then decay into a proton, electron, and anti-neutrino with an average half-life of 10.4 minutes (Kaeri, 2000). Neutrons are emitted through a variety of nuclear reactions including capture of an electron by a nucleus, fission, and (α, n) reactions. Neutrons are also classified by the amount of energy they possess, where a high energy (i.e. MeV range) neutron is said to be a *fast neutron* and lower energy neutrons fall into a spectrum and labeled as epithermal, thermal, cold and so on. Neutrons with energy less than 1 keV, including thermal neutrons, have a weighting factor of 5. Fast neutrons with energies ranging from 0.5 to somewhat above 1 MeV have a weighting factor of 20, and above this energy the weighting factor drops back to 5. (LaMarsh, 2001)

Unlike alpha particles, neutrons are categorized as indirectly ionizing radiation and as such major reactions only occur when a neutron directly interacts with a target nucleus. Neutrons also tend to be very penetrative through most materials. The energy lost by neutrons interacting with the nucleus of an atom can be determined using the following equation:

$$E' = \frac{1}{2}(1 + \alpha)E, \qquad \textbf{(2.5)}$$

where E’ is the average energy of the neutron after collision, E is the energy is initial energy of the incident neutron, and α is known as the collision parameter. The collision parameter is defined as

$$\alpha = \left(\frac{A-1}{A+1}\right)^2, \quad \textbf{(2.6)}$$

where A is the atomic mass of the nucleus involved in the collision. It follows that for collisions with low mass nuclei, more energy will be transferred per collision event from the neutron to the nucleus. For example, a neutron colliding with the nucleus of a hydrogen atom with A = 1 atomic mass results in approximately half of the neutron energy being lost. After several collisions a neutron will lose most of its initial energy. (LaMarsh, 2001)

Typically, neutron interactions with the nuclei of atoms are sorted into five unique categories: elastic scattering, inelastic scattering, (n, *x*n) reactions, (n, γ) reactions, and (n, p) or (n, ion) reactions. In most neutron interactions with a given target nucleus, the neutron and nucleus will, after the initial collision, form an intermediary compound nucleus in an excited state. The compound nucleus will be unstable and decay resulting in one of the four reaction types listed above. (LaMarsh, 2001)

Elastic scattering occurs when neutrons passing through a medium then collide with the nuclei of the atoms of the medium with a certain probability, or cross section, according to the energy of the incident neutron. These neutrons impart recoil energy to the nucleus equal to the energy lost by the neutron in the

collision as governed by equations 2.5 and 2.6 above. This reaction typically results in the excitation or displacement of atoms within the interacting medium. In the case of the inelastic collision, an incident neutron will collide with the target nucleus and impart its energy to the nucleus. However, the neutron will become absorbed into the nucleus thereby increasing its atomic mass by the weight of one neutron. The end result of this type of reaction is that the nucleus becomes displaced within the medium and can emit a γ ray. (Was, 2007)

In the case of the (n, xn) reaction type, an incident neutron will collide and reaction with a nucleus and then *x* number of neutrons will be released. Most reactions of this type result in 2 neutrons being released and as such the reaction is commonly written as an (n, 2n) reaction. The (n, γ) reaction type is a reaction where an incident neutron will result in the excitation of the nucleus and subsequent emission of a γ ray photon. (Was, 2007)

The final type of neutron-nucleus interaction is the (n, p) or (n, ion) type of reaction. The majority of reactions of this type are endothermic, with exceptions being reactions involving a few light nuclei such as the $^{10}B(n, \alpha)^{7}Li$ reaction. These reactions will not occur below a certain threshold energy dependant on the target nucleus; however, the interaction cross-section for this reaction type tends to be small even for neutrons above the required threshold energy. The cross-sections tend to be even smaller for reactions releasing heavier ions. (LaMarsh, 2001)

In the case of crystalline metals, an incident neutron will interact with an initial atom within the lattice structure of the metal and cause this atom to become

displaced from its initial position within the lattice. This initial atom is known as the Primary Knockoff Atom (PKA) and is typically the progenitor of a cascading reaction resulting in the displacement of many more atoms. This cascading results in damage to the overall structure of the crystal lattice (Was, 2007). This behavior can be modeled using computer algorithms to predict the severity and extent of irradiation damage by a flux of neutrons. However, polymers are not as well ordered in structure as most metals. This means that it becomes difficult to make many generalizations about the behavior of polymers under neutron irradiation. At the least, due to the properties of collision listed in the above equations, for a collision with a nucleus of ^{12}C, which along with hydrogen composes most of the mass of polymers, a neutron will lose approximately 14% of its energy per collision. (LaMarsh, 2001) This means that incident neutrons will transfer significant energy to the components of polymers and will likely result in destruction of large portions of the polymer matrix.

Previous neutron damage studies on polymers suggest that the polymers Hypalon® and polyurethane degrade at least somewhat under a flux of neutrons (Casey, 2004 and Griffen, 2006). The properties of nylon 6 under neutron fluence levels of 10^6 to 10^8 neutrons cm^{-2} were also studied. It was determined that the mechanical properties of nylon 6 degrade continuously under this level of irradiation (Fadel *et al.*, 1989). Nylon 6,6 has also seen review under high dose neutron irradiation. The effect of this irradiation was that the nylon experienced an increase in the rubberization of the material as well as an increase in the elastic modulus possibly resulting from an increase in the cross-linking of intermolecular

bonds within the polymer matrix (Deeley, 1957). However, studies on nylon 6,6 samples approximating the casing of the Fire Foe™ system to be used within gloveboxes is still pertinent and of specific interest in this study.

2.2.3 Gamma Ray Radiation

Gamma rays and x-rays are classes of photon irradiation. Gamma rays are emitted from the decay or de-excitation of atomic nuclei from a higher energy state to a lower or ground state. Gamma rays have higher energy than X-rays, which are emitted through de-excitation of electrons in the orbital shells surrounding atomic nuclei. Gamma ray photons are highly penetrative through many materials, and typical shielding to protect against them requires the usage of highly dense material such as lead. (LaMarsh, 2001) Gamma irradiation is often used in industrial and commercial processes to induce cross-linking within polymers to increase tensile properties and produce a material of higher strength. These strengthened polymers are often used in textiles or for biomedical applications (Bhattacharya, 2000).

Nylon polymers have been extensively studied under various levels of gamma irradiation. Nylon-6/polypropylene polymer blends were subjected to low level gamma irradiation dose to the effect that the polymer was strengthened. It was determined that adding more polypropylene to the nylon-6 polymer further enhanced the degree to which irradiation effected the material. (Chen, 2011) Nylon-6 was also subjected to much higher gamma doses in the range of 10-60 Mrad. This high level of dose had the effect of continual degradation of tensile

strength with increasing dose (Ellison *et al.*, 1984). Studies on the effect of the degree of crystallinity of polymers under irradiation have yielded results suggesting that polymers of lower crystallinity have increased susceptibility to material changes caused by gamma irradiation (Olivares *et al.*, 1996). Alpha particle and neutron radiation comprises the majority of glovebox radiation incident on the Fire Foe™ system meaning that gamma ray dose, while not unimportant, is a secondary concern.

2.2.4 Proton and Beta Particle Radiation

Protons and beta particles, also known as electrons, in addition to neutrons are the basic building blocks of all atoms. Little to no quantities of either of these radiation types are produced in gloveboxes containing plutonium, but since there have been irradiation studies with nylon under them, then they shall be mentioned in brief. Proton radiation is typically produced through (n, p) reactions where a neutron will interact with a nucleus and eject a proton. Protons are singularly charged, positive ions and behave somewhat similarly to alpha particles (LaMarsh, 2001). High dose proton radiation causes nylon to become very brittle and fracture more easily under an applied stress (Ellison, 1984). Beta particles are singularly charged negative ions that also have much less mass than protons or neutrons (LaMarsh, 2001). Beta particle irradiation experiments are usually conducted using charged particle beams to apply dose to a target. Previous work has used beta particle beams to induce cross-linking in nylon 6,6 films and

thereby increase tensile strength and produce a permeable polymer membrane (Linggawati, 2009).

Chapter 3: Experimental Facilities and Methods

During the course of this project, various methodologies were explored to simulate radiation doses which samples of nylon 6,6 material would receive as part of the casing of the Fire Foe™ fire suppression system contained within plutonium gloveboxes at Los Alamos. Following initial characterization of the Fire Foe™ system to determine the proper size of nylon tensile specimens, specimens were obtained from sheets of nylon 6,6. The dose from alpha particles on the nylon material from plutonium in a glovebox was determined using both SOURCES 4C and MCNPX computational programs. It was determined that in order to irradiate the samples with an appropriate dose of alpha particles, then an alpha particle ion beam would be required such that irradiation times would not be excessive. A set of samples were also subjected to 6 months of continual neutron irradiation using a PuBe source. The neutron irradiation duration was chosen due to time constraints for the completion of the experiment.

3.1 ALPHA ION BEAM TESTING

It was quickly apparent at the beginning of this investigation that there would be only 2 modes of alpha particle irradiation available for use. The first was to use a low dose point source consisting of a high mass radioactive element. Unfortunately, using the low dose source would require extremely long irradiation times and unusual rigging in order to adequately irradiate nylon tensile samples according to the amount of dose expected from time in a glovebox. The second

and ultimately chosen method was in using an alpha particle ion beam located in the Material Science Laboratory facility at LANL.

3.1.1 Computational Determination of Dose

Prior to conducting any irradiation experiment, it was necessary to determine the proper dose from alpha particles that should be applied to samples of the nylon 6,6 material. This required the use of a computational model simulating conditions within the glovebox referred to as a worst case scenario, or rather a glovebox with a high dose and capability of delivering that dose from alpha particles to materials distributed throughout the glovebox. The radioactive source in gloveboxes can take on a few disparate forms depending on the applications and experiments being explored within the glovebox. In the so called worst case scenario, this glovebox has a source composed of plutonium oxide dispersed as a dense fog of particulates throughout the whole of the glovebox. These particulates accumulate on surfaces within the glovebox and coat them with a layer of the plutonium oxide dust. Using these constraints as a basis, a computational model was then constructed using SOURCES 4C and MCNPX (Wilson *et al.*, 2002; Pelowitz, 2008).

3.1.1.1 SOURCES 4C Code

The SOURCES 4C code was used first for this experiment in order to develop a characterization of the radioactive plutonium source as it exists in close contact with the surface on the inside of the glovebox. SOURCES 4C is a

computational code that was developed in order to solve for neutron production rates and spectra resulting from (α, n) reactions, spontaneous fission, and delayed neutron emission due to the decay of radioisotopes. The code is limited to solving only 4 types of (α, n) reaction rate problems: homogenous media, two-region interface problems, three-region interface problems, and the case of a monoenergetic beam of alpha particles incident on a slab of material and subsequent (α, n) reactions. In the case of the homogeneous media, a radioactive alpha particle source is mixed in with some low-Z target material. The region interface problems are constructed with a slab of an alpha emitting radioactive source in contact with either another slab of target material or else held between two slabs of target material. (Wilson *et al.*, 2002)

In the scenario of the worst case glovebox, the problem can be approximated using the two-region interface model. In this model, the radionuclide source, ^{239}Pu in the case of the glovebox, is arranged in a slab joined at a boundary by another slab of low-Z target material. The low-Z target material is then a section of the nylon 6,6 Fire Foe™ casing and thus the target slab is a mixture of carbon and hydrogen atoms with the density of nylon. The SOURCES 4C code makes an underlying assumption that the thickness of each slab is greater than the range of alpha particles through the particular slab and that the alpha particles will travel in a straight path from the point in the source slab from which they are emitted. However, the code does take into account the probabilities that an alpha particle can be emitted in any number of given orientations. So for alpha particles emitted from the source region, half of the alpha particles will, on

average, be transmitted into the target region at some angle relative to the boundary of the two regions. The two-region model is shown in Figure 3.1. (Wilson *et al.*, 2002)

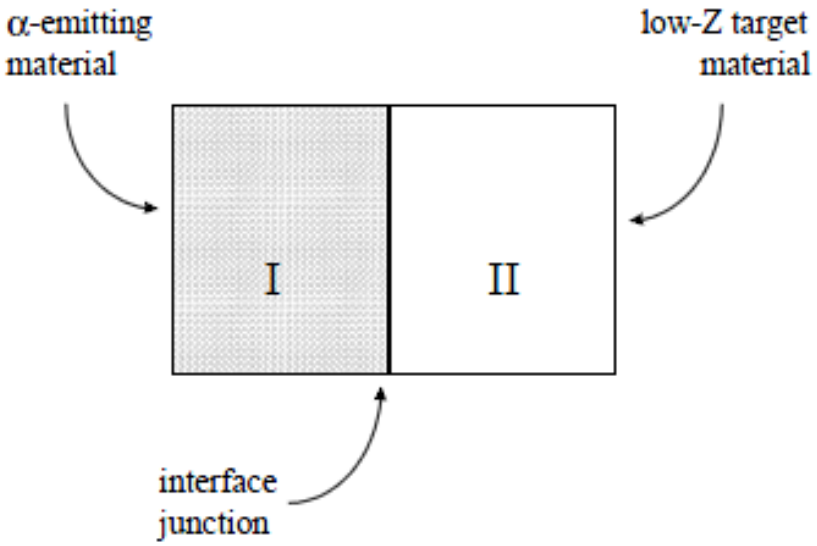

Figure 3.1: SOURCES 4C Two-Region Problem. The alpha emitting source is shown as Region I and the target is shown as Region II. (Wilson et al, 2002)

The SOURCES 4C code is often used to determine neutron production within target material slab, but in order to do so the code must first construct a table of alpha particles, sorted by energy, for the radioisotope of the source slab. The most common emitted energy of alpha particles from ^{239}Pu and ^{238}Pu isotopes was given previously as 5.157 and 5.593 MeV, respectively. However, these isotopes do not necessarily emit alpha particles only at those discrete energy levels, and as such SOURCES 4C is capable of calculating a spectrum of the number of alpha particles of each emission based on the emission probability and amount of radioisotope present within the source slab. The resulting output list is

given in the number of alpha particles emitted per cm^2. This table output information for alphas ranging from 0 to 5.6 MeV. The table of alpha particles from the source as a function of alpha particle energy determined by the SOURCES 4C code is given in Appendix A.

The maximum alpha particle energy of 5.6 MeV requires that the region of the source be no less than $1.4 \cdot 10^{-4}$ cm thick in order for region to be sufficiently thick. The total number of emitted alpha particles emitted by the plutonium source that is 1 cm^2 in area at the boundary with the target material and $1.4 \cdot 10^{-4}$ cm thick is then determined to be $1.69 \cdot 10^{7}$ Alphas cm^{-2} s^{-1}. This alpha particle emission results in energy deposition of $4.29 \cdot 10^{7}$ MeV cm^{-2} s^{-1} into the nylon material. The maximum range of the highest energy alpha particle in the nylon is determined to be $3.313 \cdot 10^{-3}$ cm in nylon 6,6.

3.1.1.2 MCNPX and Dose Calculation

The alpha particle source data obtained from SOURCES 4C was used as input in an MCNPX code model in order to determine the dose from alpha particles onto nylon 6,6 material present within a glovebox. MCNPX is a Monte Carlo based code designed to model radiation transport of multiple radiation types through material for a range of particle energies. The code is applicable to a plethora of scenarios including modeling of high energy dosimetry, designs of shielding, and nuclear criticality safety among other applications. (Pelowitz, 2008)

The MCNPX code can used to create a 3-dimensional model of a complete glovebox with sources placed as needed. This model can be much more complex than the simple modeling of the SOURCES 4C code and as such offers MCNPX a much higher degree of flexibility for solving problems. It is even possible to construct a multi-layered surface in order to examine the penetration depth and dose at each layer for a given type of radiation. For the purposes of this experiment, the code was used to construct a model similar to the SOURCES 4C two region problem using the aforementioned source data; however, the nylon region was dissected into 5 separate layers in order to model how the alpha particle radiation would be expected to transmit through the material. Using MCNPX, the alpha particle dose rate into nylon 6,6 within the worst case glovebox was determined to be $6.2 \cdot 10^{9}$ Rad cm^{-2} yr^{-1} or 196.47 Rad cm^{-2} s^{-1}. The majority of the alpha particle deposition was determined to be in the uppermost layer in direct contact with the source region.

3.1.2 Selection of Alpha Particle Irradiation Source

In order to achieve results within a reasonable timeframe, it was necessary to select a source of alpha particles that would be able to apply the required dose to the nylon 6,6 material at a rate commensurate with or greater than the dose rate present within the glovebox. Griffen (2006) had previously attempted to use a low activity ^{244}Cm alpha particle point source. Curium-244 decays primarily through emission of alpha particles to ^{240}Pu with a half life of 18.1 years with an energy of 5.9 MeV per particle. This alpha particle energy is somewhat higher

than the average energy of alpha particles released by the plutonium source. The specific ^{244}Cm source had an activity of 10 μCi with a 5 mm active area diameter resulting in an effective dose output of 100 rads per minute of alpha particle irradiation. The largest source commercially available at the time of this experiment was 0.1 μCi, which is significantly less strong than the source used by Griffen (2006). However, there are numerous problems in using such a point source not the least of which is the requirement of a special apparatus to ensure equal distribution of dose across multiple samples. Such a source would also require extremely long irradiation times in order to properly model the dose levels samples would receive inside a glovebox. (Griffen, 2006)

Given that irradiation using an alpha particle point source would not be suitable to achieve the objectives of this experiment, it was then determined that an alpha particle ion beam would be used instead. Ion beams are regularly used to quickly irradiate material under a high dose rate or fluence of various radiative particle types including alpha particles. For example, a beam of singly ionized alpha particles, He^+, has been used previously to chemically modify PVC into a conducting polymer to great effect. In this case, a beam of 1 MeV alpha particles was introduced onto a PVC polymer target with a fluence of 10^{15} He^+ ions cm^{-2} in order to promote the growth of free radicals within the PVC and stimulate chemical alteration. (Davenas, 1995) The dose rates capable of being produced by ion beams are far greater than the dose rates that can be supplied from alpha particle point sources. Thus, an alpha particle ion beam is then the only

reasonable method for irradiating polymers to sufficiently model radiation damage within high dose gloveboxes within a short timeframe.

3.1.3 Ion Tandem Beam Facility

The ion beam facility chosen for this experiment was the Ion Beam Materials Laboratory within the Materials Science Laboratory located at Los Alamos National Laboratory. This particular ion beam has been used previously with great success to irradiation experiments on thin polymer films by Murphy *et al* (2003). In this instance, the ion beam generated a fluence of 7.5 MeV He^{++} ions with a beam current of 12.5 nA delivered to a target area of 3 cm^2. These alpha particles were passed through a 10 μm Havar foil to reduce the ultimate energy of the beam particles incident on the target material to 4.25 MeV. The dose level applied by the beam to the target films used during this particular experiment were recorded to be on the order of 100s of Mrad. (Murphy *et al*, 2003) Given the success of this prior experiment and the opportune location of the ion beam facility at Los Alamos National Laboratory, this facility was the optimal choice for use in the current experiment on nylon.

The facility employs a 3.2 MV tandem ion accelerator with a 200 kV ion implanter in conjunction with multiple beam lines in order to generate high fluence rate of the desired particle type for a given experiment. The ion beam is able to generate streams of protons with energies ranging from 200 keV to 6.4 MeV, alpha particles with energies from 200 keV to 9.6 MeV, and heavy ions with energies that range from 200 keV to 20 MeV. Alpha particles emitted in this

range are below the relativistic energy limit near 37 MeV. The tandem ion beam accelerator is capable of running at currents between several pA to the range of a few μA, which is equivalent to a few mCi to several thousand Ci, respectively, from a radioactive source of alpha particles. This makes the ion accelerator an extraordinarily useful tool for irradiating targets quickly and to high dose levels. Several analytical tools are also available in combination with the main beam line including Rutherford backscattering spectroscopy, nuclear reaction analysis, and particle induced x-ray emission. These tools are used to measure changes to samples caused by irradiation from the beam line. Samples are capable of being irradiated through the range of temperatures from -190 to 500 °C. Figures 3.2 to 3.6 below show the pathway a beam generated at the ion beam facility ending at the target chamber. (Wang, 2006)

Figure 3.2: Tandem Ion Accelerator. This is the principle accelerator chamber where alpha particles are brought to the appropriate energy and fluence rate as required for a given experiment. (Wang, 2006)

Figure 3.3: Primary Alpha Particle Beam Line. The tandem ion accelerator feeds into this section of the beam line where the ion beam is further constrained prior to introduction to the sample chamber.

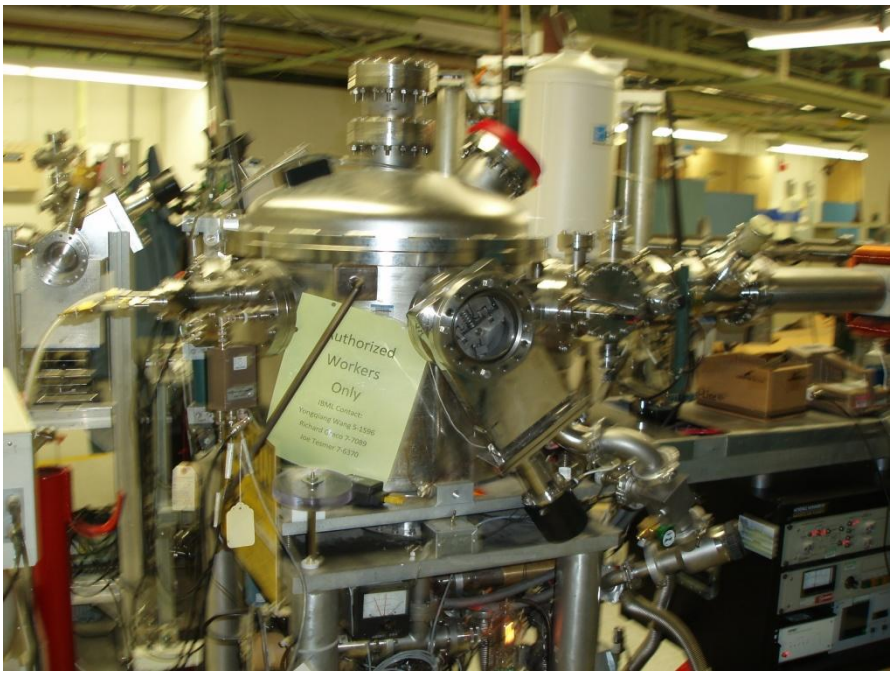

Figure 3.4: Exterior of the Sample Chamber. The alpha particle ion beam supplies into this vacuum chamber and onto samples to complete irradiation.

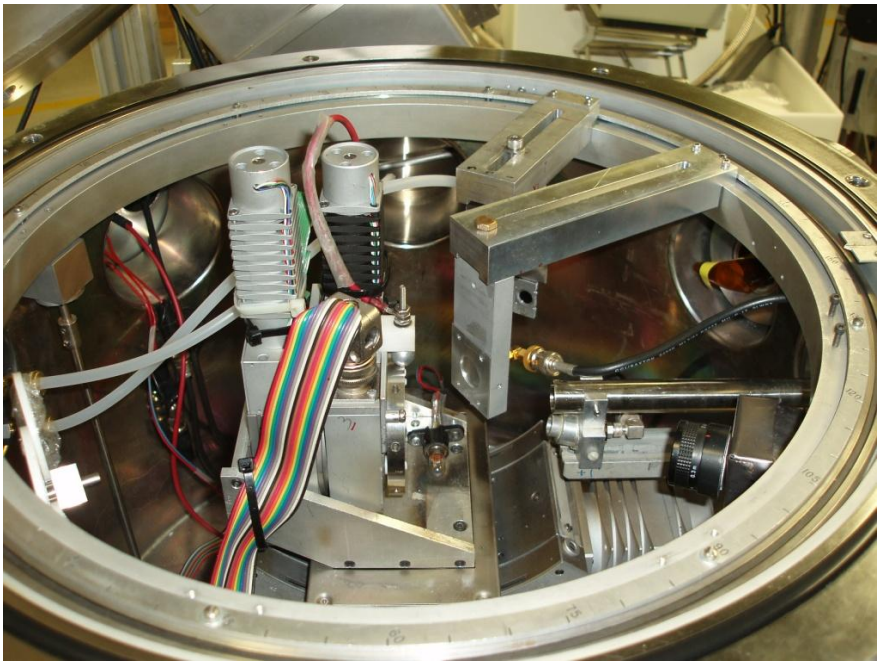

Figure 3.5: Interior of the Sample Chamber. The inside of the vacuum chamber with the lid removed. The sample target sits affixed to the central pylon and is rotated to be irradiated by the ion beam.

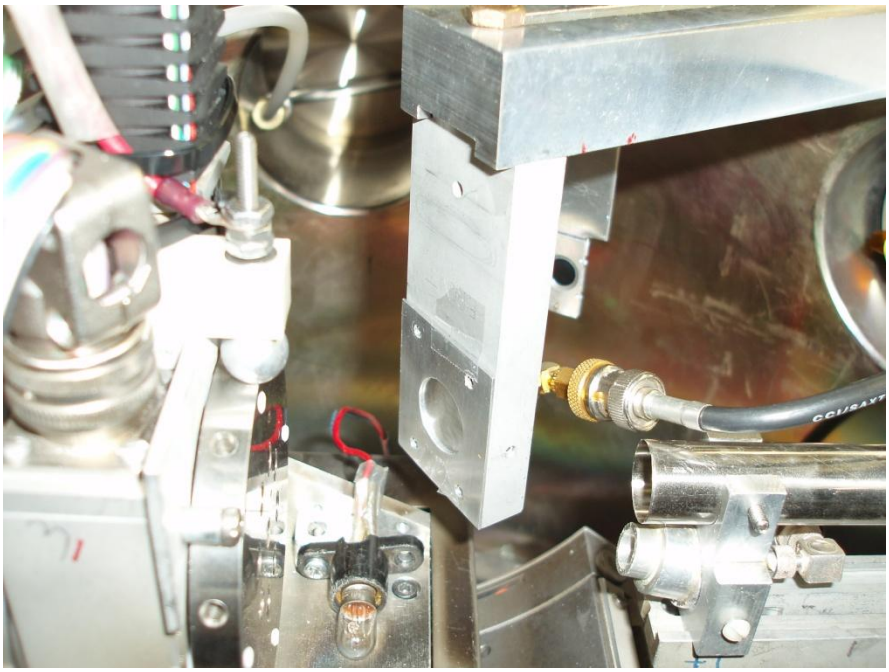

Figure 3.6: Close-up of the Interior of the Sample Chamber. An empty sample target disk is loaded onto the central pylon on the lower left. The ion beam exits from the steel tube on the lower right to irradiate samples.

For the purposes of this experiment, nylon 6,6 samples were irradiated at the LANL ion beam facility using a beam with 90 nA current output with a terminal voltage of 2.225 MV. The beam emitted alpha particles with an energy of 4.5 MeV per particle. The resulting beam fluence rate was $3.12 \cdot 10^{11}$ He^{++} ions s^{-1} onto a target area measuring 1.7 cm in length by 1.5 cm in width or 2.55 cm^2. This fluence rate translates into a dose rate from the beam of $3.6 \cdot 10^6$ Rad s^{-1} incident on the target and allowing samples to be aged at an accelerated rate of $1.7 \cdot 10^3$ seconds in the beam per one year in the worst case glovebox. In order to ensure that each section of the target would receive an equal amount of dose, a scanning technique was used in which the beam was passed over the target area where the beam was swept to the right and left of the target at a constant rate. This scanning technique was required due to the relatively large size of the sample target. Figures 3.7 to 3.9 show the nylon 6,6 specimens loaded on a target disk and then being placed and viewed within the sample chamber.

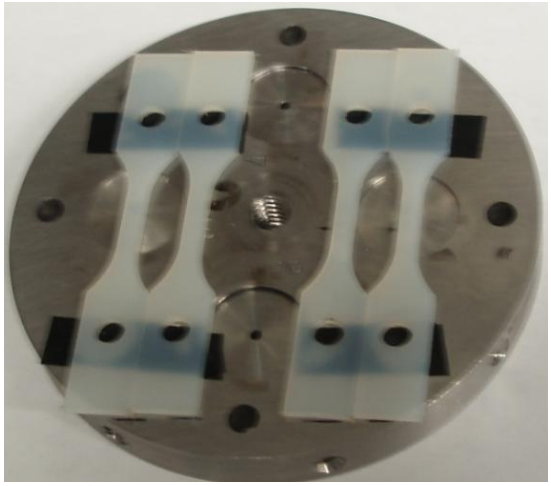

Figure 3.7: Nylon 6,6 Samples Loaded on Target. Two sets of nylon 6,6 samples are loaded onto a stainless steel target. The nylon samples are affixed to the target with double sided carbon tape.

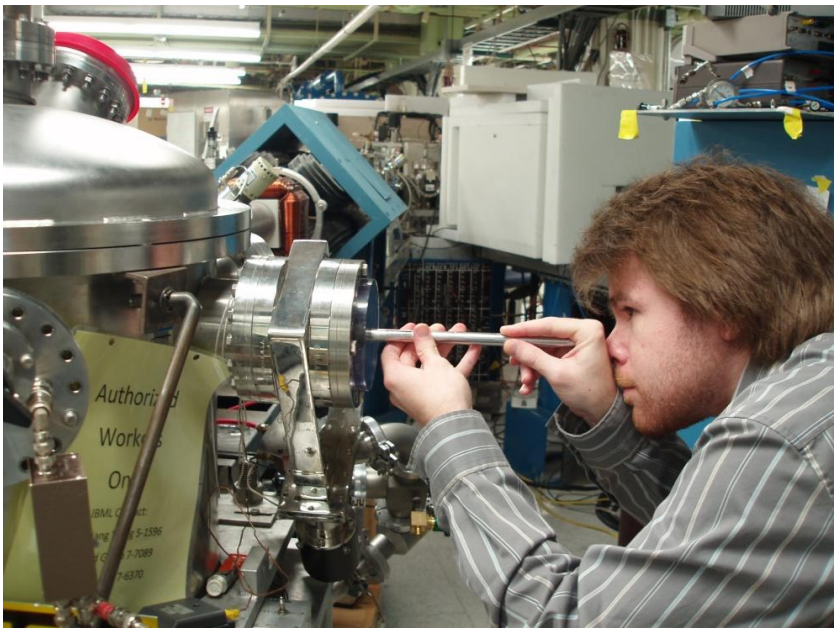

Figure 3.8: Sample Loading. Here the target disk with samples affixed is being loaded into the vacuum chamber. The vacuum within the chamber is maintained through a series of pressure seals and valves.

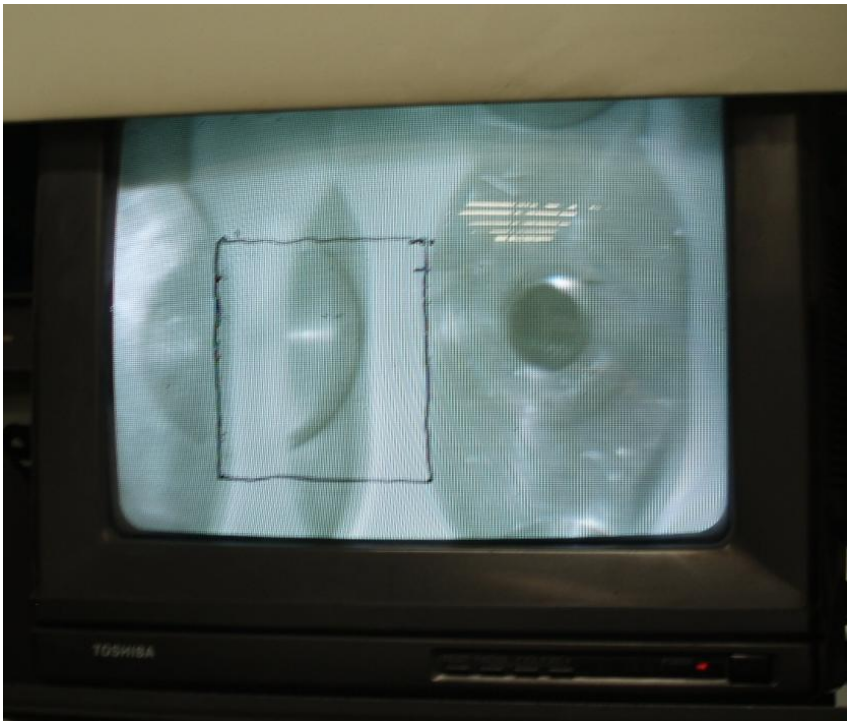

Figure 3.9: Samples in Beam. The samples are viewed with a closed circuit television feed within the vacuum chamber. The irradiated area is outlined as the black square on the screen.

3.2 NEUTRON IRRADIATION EXPERIMENT

The second source of radiation damage of interest within gloveboxes in this experiment comes from neutrons. The neutron radiation damage experiment was conducted using a plutonium beryllium, or PuBe, neutron source at the Nuclear Engineering Teaching Laboratory on the University of Texas Pickle Research Campus. This experiment closely mimics previous work conducted by both Casey and Griffin (Casey, 2004 and Griffin, 2006).

The neutron source is housed within stainless steel and tantalum casing and is composed of a homogeneous mixture of alpha particle emitting ^{239}Pu and the low-Z material ^{9}Be. At the time of shipment in 1961, the PuBe source was rated to be composed of 39.29 grams of Be and 79.94 grams of Pu. The neutron fluence rate from the source at the time of shipment from the manufacturer was $8.82 \cdot 10^{6}$ neutrons s^{-1}.

Since the source is a homogeneous mixture, then the emission of neutrons, with respect to the centerline axis of the source, will be isotropic. Neutrons will be produced by the source when alpha particles emitted by decay of the Pu isotope have sufficient energy to overcome the Coulombic barrier of the ^{9}Be nucleus and an (α, n) reaction occurs. The Coulomb barrier for a given isotope is calculated using the following equation:

$$Barrier\ (MeV) = \frac{Z_\alpha Z_n e^2}{r_0 (A_\alpha^{\frac{1}{3}} + A_n^{\frac{1}{3}})}, \qquad \textbf{(3.1)}$$

where e^2 is 1.44 MeV·fm, r_0 is 1.25 fm, Z_α and Z_n is the atomic number of an alpha particle and the given isotope respectively, and A_α and A_n is mass number of the an alpha particle and the given isotope. Using the above equation yields a Coulomb barrier of approximately 2.6 MeV for ^{9}Be. Given that the energy of the primary alpha particles emitted from ^{239}Pu ranges from 5.1 to 5.2 MeV, these alpha particles are then capable of overcoming the coulomb barrier of ^{9}Be, interacting with the nucleus, and producing subsequent neutrons. The average yield of neutrons from ^{239}Pu(α,n)^{9}Be reactions is 80 neutrons for every 10^6 alpha particles emitted from ^{239}Pu. (Shultis, 2000)

The neutron source was manufactured with a measured activity of 5 Ci in November of 1961. The source information is listed below in Table 3.1:

Table 3.1: Specifications of the PuBe Neutron Source.

Parameter	Specification	Units
Source ID	M799	
Source Type	^{239}PuBe	
Source Container	Stainless Steel	
Source Activity	5000	mCi
Manufacture Date	November, 1961	
Age	50.28	yrs
Current Activity	4992.8	mCi
Current Activity	1.847E+11	Bq
Mass ^{239}Pu	80.5	g
Source Strength	5.15E+06	n/s
Avg. Neutron Energy	4.5	MeV
Max Neutron Energy	10.74	MeV

Neutrons emitted from the PuBe source have an average energy of 4.5 MeV and a maximum energy of 10.74 MeV. Neutrons are emitted from this source in a wide energy spectrum as shown below in Figure 3.10.

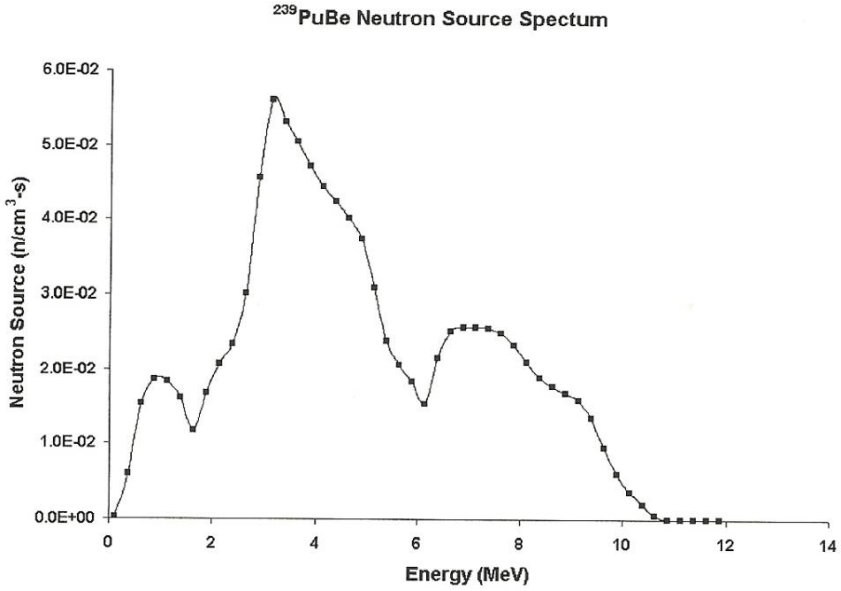

Figure 3.10: PuBe Neutron Source Spectrum. The neutron spectrum was created using SOURCES 4B by Casey for the PuBe source in 2004. A similar spectrum was created by Griffin in 2006. (Casey, 2004; Griffin, 2006)

3.2.1 Neutron Irradiation Apparatus

The PuBe neutron source was placed into a stainless steel container and set such that the source and nylon samples would be held in a fixed positions relative to each other. This was done to ensure that all the samples being irradiated would be irradiated uniformly with respect to one another. The sample holder was then placed into a larger paint can container constructed from stainless steel and aluminum. The secondary container serves as an additional barrier to external environmental conditions and also serves to limit exposure to the neutron source during the insertion and removal of the source from the sample holder. This paint can container with the source and samples loaded in was lowered into a 20 foot, or 6.1 m, deep storage well located in the reactor bay of the TRIGA

experimental reactor at NETL. This well is commonly used for the storage of radiological hazards, such as long term storage of spent nuclear fuel rods, and high radiation sources and experiments. At the time of this experiment, the well contained several spent fuel rods. Since these fuel rods emit copious amounts of gamma ray radiation, then it was necessary to add additional lead shielding to the neutron irradiation apparatus to attenuate these gamma rays. The sample holder and outer container are shown in Figures 3.11 and 3.12.

Figure 3.11: Sample Holder with Samples. Above is the sample holder loaded with several samples; the center of the holder is empty but is designed to fit the PuBe neutron source. The samples are affixed to the holder with Kapton tape.

Figure 3.12: Sample Holder and External Container. The sample holder from Figure 3.11 is shown on the lower right. This holder is placed into the larger paint can container and then the source is placed in the center of the holder in order to limit potential exposure risks.

The above equipment was constructed for previous experiments conducted by Casey (Casey, 2004). This equipment was created at NETL by University of Texas staff whose assistance allowed this experiment to proceed. However, the apparatus required a slight modification in order to attenuate gamma ray radiation from the spent fuel rods placed in the well. This means that the apparatus needed extra lead shielding attached to the bottom of the outer container so that gamma rays emitted below the container would be attenuated and not interfere with the results of the experiment. The choice of lead shielding, both in amount and

placement, was limited by both total weight and available selection of lead bricks. This modification is shown below in Figure 3.13.

Figure 3.13: Modified Neutron Apparatus. The apparatus has added lead shielding on the bottom of the outer container. The lead shielding is held to the container using a rope basket made from a nylon polymer.

3.2.2 Neutron Activation and Gold Foil Analysis

In order to experimentally determine the activity of the neutron source, it was necessary to conduct neutron activation analysis experiments on gold foil. Neutron activation analysis (NAA) is a technique used to determine the isotopic content of a material by bombarding parent isotopes within the material with neutrons to create radioactive isotopes. These radioactive isotopes will then

decay, typically with emission of a gamma ray, to a more stable isotope. These decays are then counted to determine the relative abundance of a particular parent isotope within the material.

Principally, there are two methods used to determine the amount of an isotope within a material: the absolute and comparator methods. The comparator method utilizes precise standards, such as those supplied by NIST, to compare with the unknown material of interest. The absolute method is typically used when standards are either unavailable or too expensive for use in NAA. The absolute and comparator methods are given in equations 3.2 and 3.3 below, respectively.

$$A = \varphi\sigma\left(\frac{m}{M}\right)N_A SDC\theta P_\gamma \varepsilon, \quad \textbf{(3.2)}$$

$$C_{sa} = C_{st}\left(\frac{A_{sa}}{A_{st}}\right)\left(\frac{D_{st}}{D_{sa}}\right)\left(\frac{C_{st}}{C_{sa}}\right)\left(\frac{W_{st}}{W_{sa}}\right), \quad \textbf{(3.3)}$$

where:

- A = activity
- φ = flux
- σ = cross-section
- m = mass
- M = atomic mass
- N_A = Avogadro's number
- S = [1 – exp(-λt_i)], saturation buildup, t_i is irradiation time
- D = exp[-λt_d], decay correction, t_d is the decay time after irradiation
- C = [1 – exp(-λt_c)], counting time decay correction, t_c is the counting time
- θ = relative natural abundance of the activated isotope

- P_γ = probability of photon emission
- ε = efficiency of the detector
- W = weight of the sample

Here the subscripts (sa) and (st) designate the unknown sample and the known standard. (Elving, 1972)

Neutron activation analysis can also be used to determine the strength of a source if the target activated isotope is well characterized. For this experiment, the PuBe source strength was measured using two gold foils which were irradiated using the apparatus described previously. These foils were then examined as per ASTM E262. The gold foils are composed entirely of ^{197}Au isotopes, which become ^{198}Au isotopes under neutron irradiation. ^{198}Au isotopes then decay via beta decay with a half-life of 2.7 days to ^{198}Hg with an additional emitted gamma ray of 411 keV (KAERI, 2000). One of the foils was covered using a cadmium foil due to the ability of the ^{113}Cd isotope to absorb thermal neutrons. ^{113}Cd isotopes comprise 12.22% of the total amount of naturally occurring cadmium (KAERI, 2000). This was necessary to determine the fluence of high energy or fast neutrons and the fluence of the thermal neutrons emitted by the source. The neutron absorption cross section is depicted below in Figure 3.14 from assembled ENDF data.

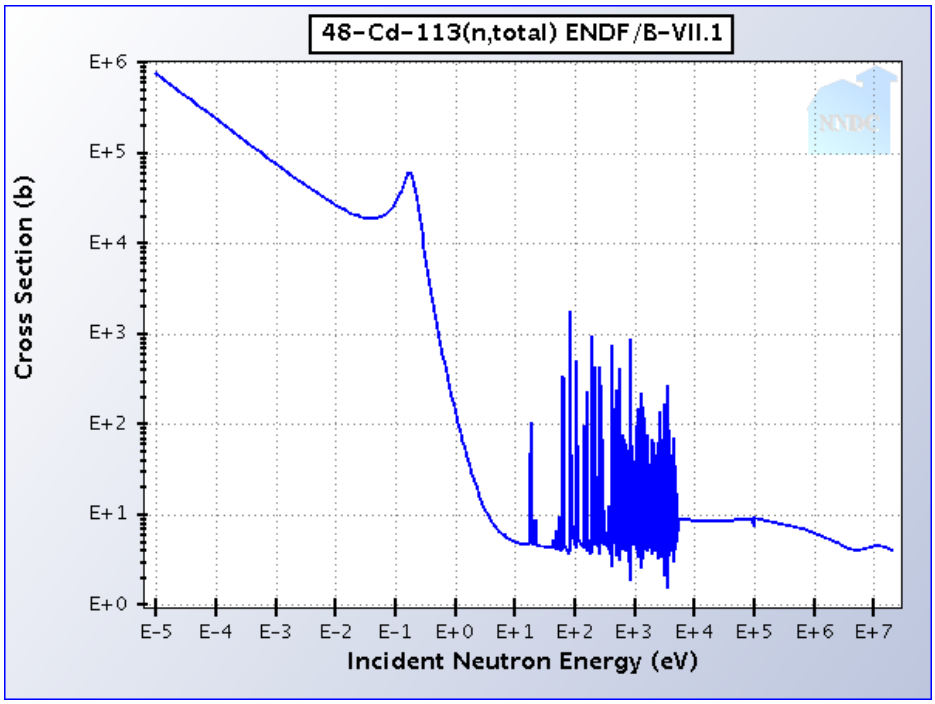

Figure 3.14: Neutron Absorption Cross Section vs. Neutron Energy for ^{113}Cd. The neutron absorption is very high for energies in the low and thermal range. (ENDF data)

The majority of neutrons incident on polymers within a glovebox will be classified as fast neutrons. Thus, it is important to ascertain the fluence of fast neutrons from the PuBe source incident on the samples. Since the two foils were placed equidistant from the source, they are expected to receive the same neutron fluence from the source. However, the cadmium covered foil is expected to be activated to a lesser degree than the non-covered foil. The foils were irradiated for 7 days before being extracted.

3.2.2.1 Gamma Ray Detection

Following irradiation, the foils were counted individually using a high purity germanium detector system. Gamma ray photons entering the detector are

registered as signal which is sent to a multichannel analyzer. This multichannel analyzer records the number of photons counted as a function of the voltage of the corresponding signal. This is interpreted using electronics and computer software into the number of photons detected against the energy of the photons. All gamma ray counting was done with the samples and sources fixed at 11 cm from the face of the detector crystal.

Prior to obtaining measurements for the gold foils, it was necessary to determine the counting efficiency of the detector. This was done by taking a well-known standard of the isotope ^{152}Eu and counting for a period of time. ^{152}Eu has several gamma ray peaks spread over the range of energies from 120 to 1400 keV, and thus making it an ideal standard to create an efficiency curve for the detector over a large energy range. The ^{152}Eu source used was manufactured with an activity of 396 kBq in July, 1995. This source was determined to have an activity of 168.8 kBq in February, 2012. The efficiency curve for the HPGe detector was created using Microsoft Excel and is shown below.

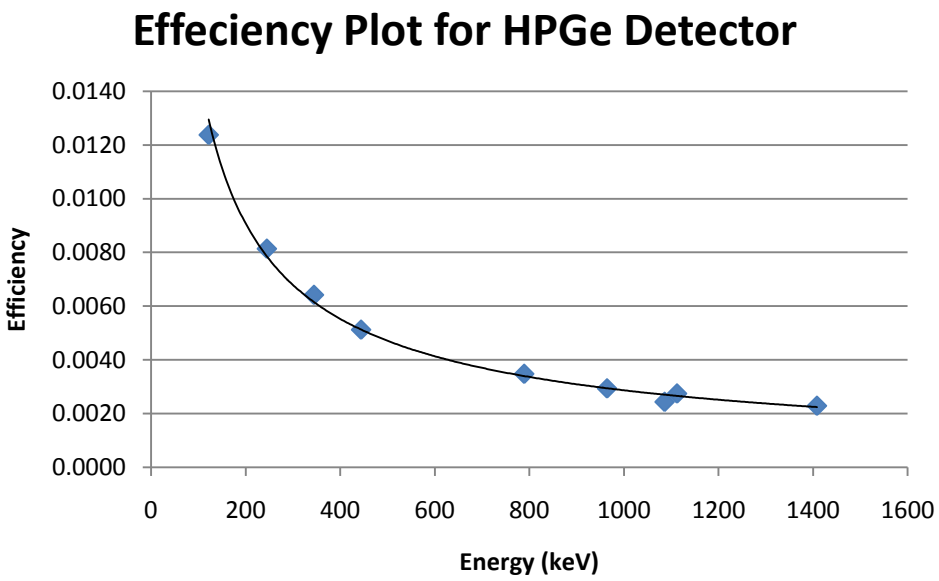

Figure 3.15: Efficiency of HPGe Detector. The efficiency of the detector is much higher at lower gamma ray energies. This is a known occurrence for HPGe and semiconductor detectors.

The foils were counted for 24 hours apiece. Counting on the bare foil began approximately 2 hours after the end of irradiation by the PuBe source. The cadmium covered foil was counted after the bare foil and approximately 28 hours after the end of irradiation. The experimentally determined flux for each foil is given in the table below, where the bare foil represents the total neutron source strength and the cadmium cover foil is the total strength minus that of the contribution from thermal neutrons.

Table 3.2: Source Strength from Gold Foils

Foil Designation	Mass (g)	Source Strength (n/s)	Std Dev (± %)
Bare (B)	0.121	1.42E+07	1.01
Cd covered (A)	0.1204	7.99E+06	1.83

It is apparent from the experimental measurements that source strength is quite high and those neutrons below the 0.4 keV cadmium cut-off produced a significant portion, greater than 50%, of the total neutrons produced. This can be explained by additional neutron fluence resulting from scattering in the system near the sample and neutron reflection at lower energies. Since the reflected neutrons are of lower energy they have a greater chance of being absorbed into the gold foils and being counted in a detector through the gamma ray decay of the activated gold.

3.3 MECHANICAL TENSILE TESTING

In order to determine the extent to which the nylon 6,6 material within the gloveboxes is damaged by irradiation, it is necessary to measure how the material properties of the nylon change under different doses of alpha particles and neutrons. The methodology of the alpha particle and neutron irradiation has been explained previously. The material properties being examined are the standard tensile properties: the tensile strength at both yield and break, the percent elongation at yield and break, and the tangent modulus of the material. Here the term "yield" refers to the point at which a stress applied to the material will cause the material to begin plastic deformation. If a material is strained beyond the yield point, then it will be unable to completely elastically rebound to its former shape. Tensile strength refers the amount of force per unit area, usually given as pounds-force per inch or psi, required to stress a material to a certain point. The tensile strength of the material is calculated by dividing the maximum load force

applied by the average original cross-sectional area of the gage length of the material specimen. If enough force is applied to a material such that the tensile strength at break is then exceeded, then the material will be ruptured by the applied force. The percent elongation is the change in the gage length relative to the original specimen gage length given as a percentage caused by an applied stress. The tangent modulus is given as the slope of the stress-strain curve modeling the behavior of a material. A typical stress strain curve is shown in Figure 3.16. (ASTM D638)

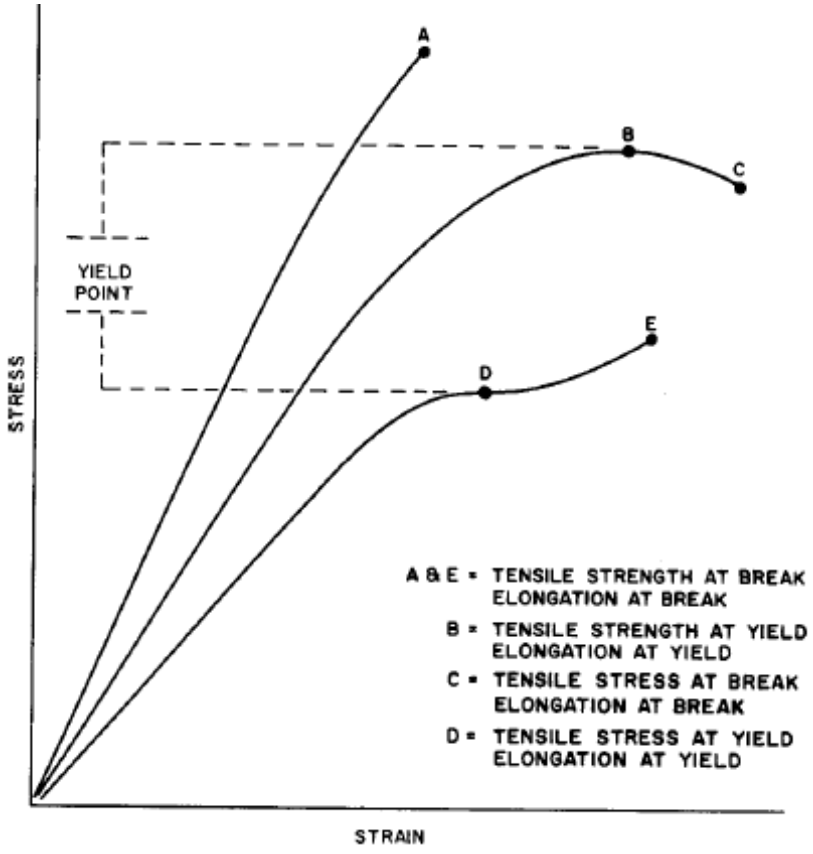

Figure 3.16: Typical Material Stress-Strain Curve. The yield point of several hypothetical materials is shown at points B and D. The stress-strain curve increases linearly until the material nears the yield point and begins to undergo plastic deformation. (ASTM D638)

Tests were conducted in order to measure the above properties for nylon samples at various levels of radiation dose and according to the American Society for Testing and Materials (ASTM) standard D638. The test specimens were cut from a 1 foot by 1 foot square tile of nylon 6,6 purchased from Plastics International. The nylon tile was 0.062" or .0157 cm in thickness which matches the thickness of the nylon casing of the Fire Foe™ fire suppression tube. The tensile samples were cut from the tile according the specifications in ASTM D638 and are depicted in Figure 3.17 below.

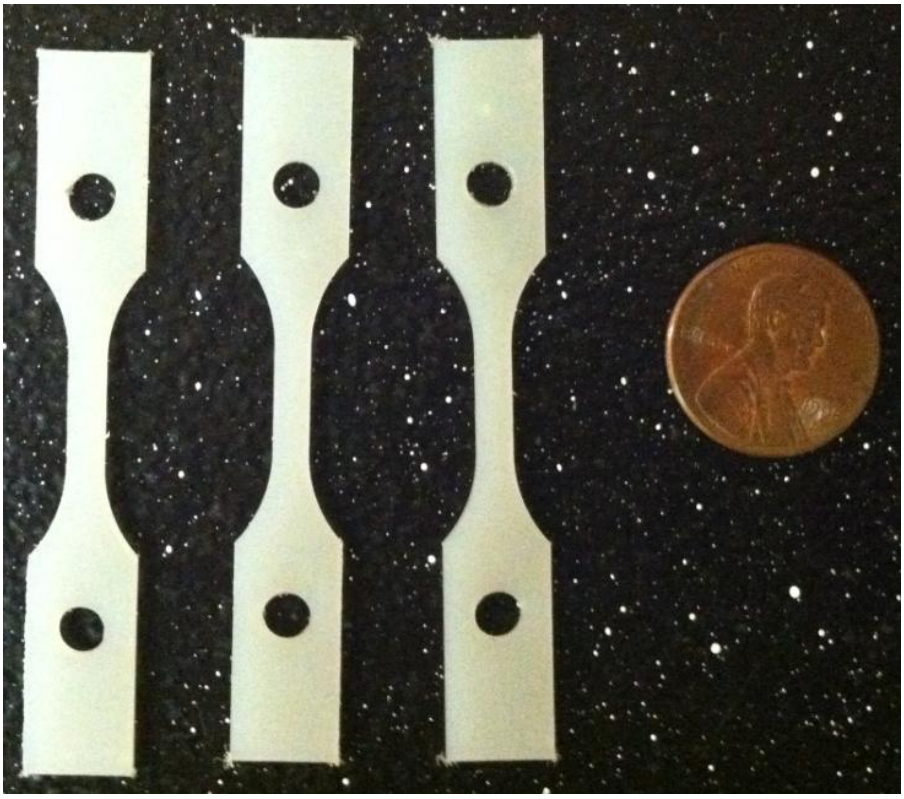

Figure 3.17: Nylon 6,6 Tensile Samples. These samples are colloquially referred to as "dog-bone" samples due to their shape. The specimens are shown with a standard U.S. Abe Lincoln penny for relative size comparison.

The tensile samples conform to the specifications for Type IV specimens as mandated for samples with thicknesses less than 4 mm. The design specifications for Type IV specimens are given below in Figure 3.18 and Table 3.3:

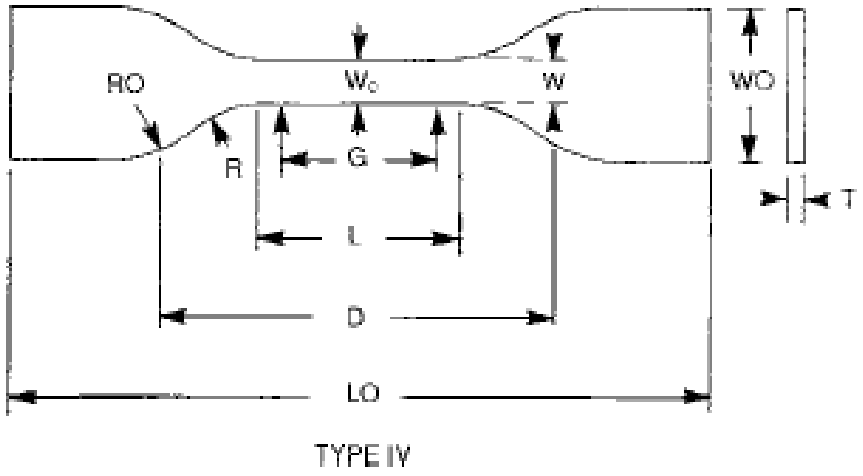

Figure 3.18: Type IV Tensile Sample Specifications. The nylon was cut to fit this shape in accordance with ASTM standards. (ASTM D638)

Table 3.3: Type IV Sample Specifications

Dimension	Value (mm)	Tolerances (mm)
W – Width of narrow section	6	±0.5
L – Length of narrow section	33	±0.5
WO – Width overall, min	19	±6.4
LO – Length overall, min	115	no max
G – Gage Length	25	±0.13
D – Distance between grips	65	±5
R – Radius of fillet	14	±1
RO – Outer Radius	25	±1

After irradiation conditioning the samples were sent to an external laboratory for tensile testing. Efforts were made to have the testing done onsite at

the University of Texas; however, those efforts did not ultimately bear fruit. The lab used for testing was Polyhedron Laboratories, Inc. located in Houston, TX.

Each testing specimen was conditioned according to ASTM D618 prior to tensile testing as specified in ASTM D638 in order to ensure that each specimen is tested under the same temperatures and humidity conditions. Each sample set requires a minimum of 5 tensile specimens in order to achieve results with proper statistical evaluation. Tensile samples are typically tested using Instron machines such as the one pictured in the figure below. Type IV tensile samples are tested at a rate of applied strain on the order of 5, 50, or 500 mm per minute. The testing speed is chosen based on the lowest of the three listed speeds that causes a rupture in a sample within ½ to 5 minutes of testing time. The testing speed was reported to be 0.5" per minute by Polyhedron Labs. (ASTM D638)

Figure 3.19: Instron Testing Machine. A typical Instron tensile testing machine used for determining tensile properties of materials such as polymers is shown. A dog-bone polymer sample is loaded and being held in place by clamps on either end of the specimen.

Chapter 4: Experimental Results

The experimentation conducted during the course of this project was centered on the change to the mechanical properties of nylon 6,6 material undergoing irradiation from both alpha particles and neutrons in order to model damage from like radiation sources within plutonium gloveboxes. The alpha irradiation work was conducted onsite at LANL and the neutron damage work was conducted at the University of Texas as described in the previous chapter. The results of these experiments are now reported in full.

4.1 ALPHA PARTICLE DAMAGE STUDIES

The alpha ion beam irradiation of the nylon 6,6 samples was conducted in June of 2012. There were a total of 50 specimens irradiated over the course of 3 days. The samples were irradiated to model doses equivalent to the time spent in the worst case glovebox for 1 month, 6 months, 1 year, 3 years, and 6 years with 10 samples per time set. The samples were irradiated in sets of two specimens per run of the ion beam with two sets of samples, a total of 4 individual specimens, loaded into the vacuum chamber at any given time as shown in Figure 3.7. The samples were irradiated at a rate within the beam such that 2 minutes and 10 seconds was equivalent to 1 month within the glovebox.

The mechanical properties of the nylon sample sets following alpha particle irradiation are shown below in Tables 4.1 and 4.3. The corresponding standard deviations for the values in Tables 4.1 and 4.3 are given in Tables 4.2

and 4.4, respectively below. The full data from each tested specimen is given in Appendix B.

Table 4.1: Alpha Particle Irradiation Results

Averages	Tensile Strength		% Elongation		Tangent
Dose Equivalent (yr)	at yield (psi)	at break (psi)	at yield	at break	Modulus (psi)
0	8704.8	7805.8	28.5	99.3	309,788.5
0.083	7951.9	7315.6	31.1	120.2	165,908.9
0.5	7964.2	7112.9	34.4	86.5	159,650.6
1	8059.5	7105.7	29.4	77.4	209,474.6
3	8182.9	7418.8	29.5	66.3	247,224.4
6	8174.3	7091.9	27.5	65.4	227,077.4

Table 4.2: Standard Deviations in Alpha Particle Irradiation Results

Std Dev	Tensile Strength		% Elongation		Tangent
Dose Equivalent (yr)	at yield (psi)	at break (psi)	at yield	at break	Modulus (psi)
0	147.9	134.7	5.1	13.5	16,131.5
0.083	261.1	322.5	2.3	57.1	5391.6
0.5	283.7	330.6	4.4	14.2	52,822.5
1	83.8	179.7	6.5	16.7	61,919.9
3	138	44.2	2.4	8.9	89,423.4
6	65.4	389.9	4.8	25.3	126,421.2

Table 4.3: Alpha Particle Results in MPa

Averages	Tensile Strength		Tangent
Dose Equivalent (yr)	at yield (MPa)	at break (MPa)	Modulus (MPa)
0	60.02	53.82	2135.92
0.083	54.83	50.44	1143.90
0.5	54.91	49.04	1100.75
1	55.57	48.99	1444.28
3	56.42	51.15	1704.55
6	56.36	48.90	1565.64

Table 4.4: Standard Deviations of Alpha Particle Results in MPa

Std Dev Dose Equivalent (yr)	Tensile Strength at yield (MPa)	Tensile Strength at break (MPa)	Tangent Modulus (MPa)
0	1.02	0.93	111.22
0.083	1.80	2.22	37.17
0.5	1.96	2.28	364.20
1	0.58	1.24	426.92
3	0.95	0.30	616.55
6	0.45	2.69	871.64

The non-irradiated material property values agree with previously measured book values for nylon 6,6. The data was further analyzed using standard single factor analysis of variance, or ANOVA, techniques and given in Appendix C. The data provided in tables 4.1 to 4.4 were plotted using Microsoft Excel and given in Figures 4.1 to 4.5 below.

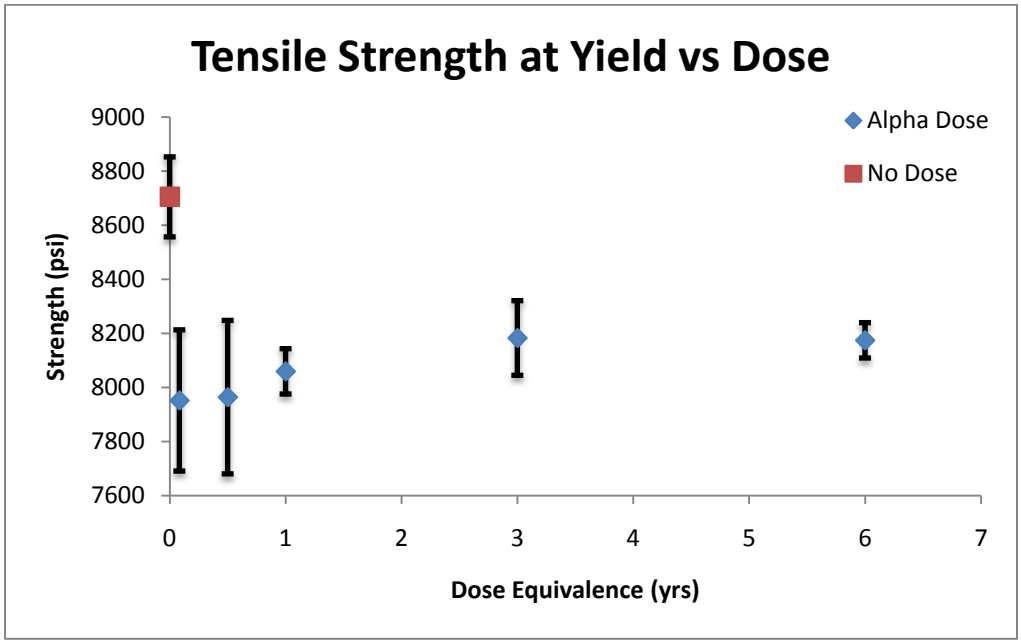

Figure 4.1: Tensile Strength at Yield vs. Alpha Particle Dose. The applied force required to bring a sample with an equivalent glovebox dose expressed as years to the yield point.

The tensile strength at yield is plotted in Figure 4.1 for doses equivalent for up to 6 years in the worst case glovebox. It is apparent that even a relatively small amount of dose applied to the nylon 6,6 samples results in a decrease in tensile strength of 600 to 1000 psi. Applying ANOVA statistics to the results shows that the alpha irradiated samples sets are distinctly differentiated from the non-irradiated set; however, for increasing levels of alpha particle dose, the differentiation of the data sets fall under the 95% confidence level. Overall, there is less than an 8.65% decrease from the initial strength level at maximum which occurs at 1 month's dose. There appears that there might be some recovery in this property at higher doses, but it is not apparent if this feature is statistically relevant.

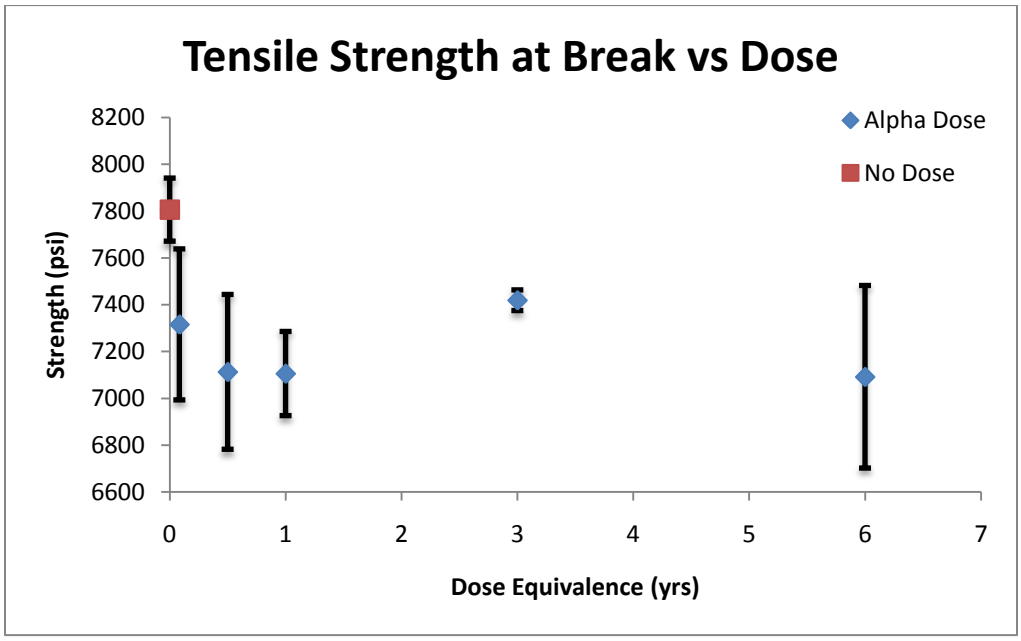

Figure 4.2: Tensile Strength at Break vs. Alpha Particle Dose. The applied force required to bring a sample with an equivalent glovebox dose expressed as years to the point of fracture of the material.

The tensile strength at break of nylon 6,6 samples is plotted in Figure 4.2 for alpha particle doses up to and including the equivalent dose of 6 years in the worst case glovebox. It is evident that the tensile strength at fracture decreases by less than 1000 psi for any applied dose. ANOVA statistics show that the non-irradiated sample set data is differentiated from the alpha irradiated sets past the 95% confidence level; however the data have a greater probability of overlap with higher dose. The maximum change in fracture tensile strength is 9.15% occurring at the maximum dose of 6 years. The average change of fracture tensile strength is 7.65% over all doses.

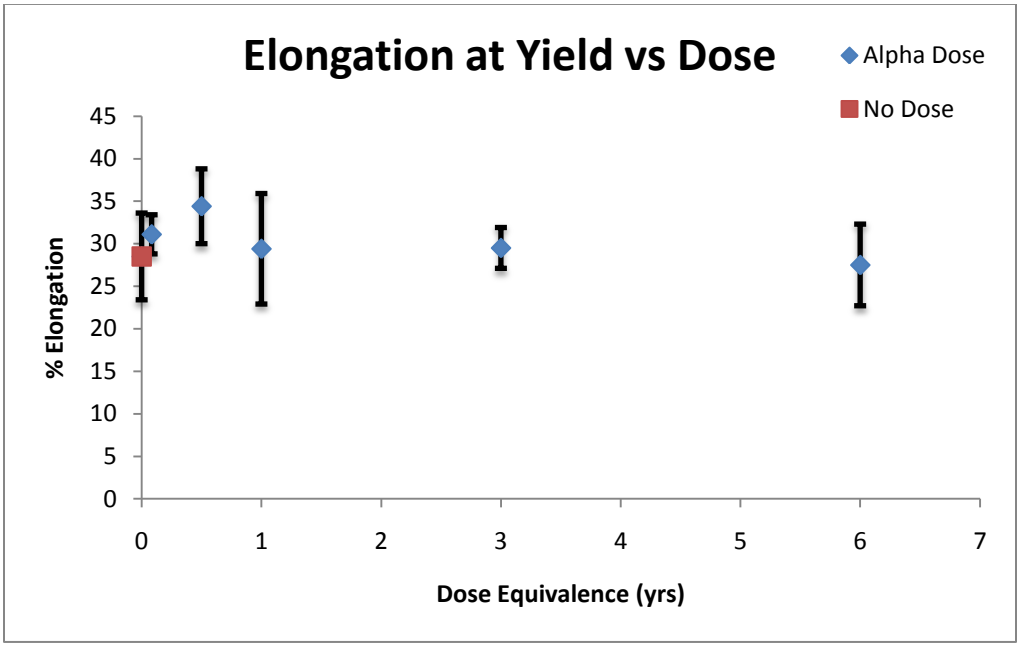

Figure 4.3: Percent Elongation at Yield vs. Alpha Particle Dose. The relative elongation from initial shape for nylon 6,6 samples under irradiation at the point where plastic deformation takes over is displayed.

The percent elongation at yield of nylon 6,6 samples is plotted in Figure 4.3 for alpha particle doses modeling equivalent time up to 6 years spent in the

worst case glovebox. The average change in elongation appears to be 8.0% among the samples. However, applying ANOVA to this data set shows that data are not statistically distinguishable regardless of the level of dose applied to the samples, meaning it is unlikely that the elongation at yield varies significantly with any level of dose.

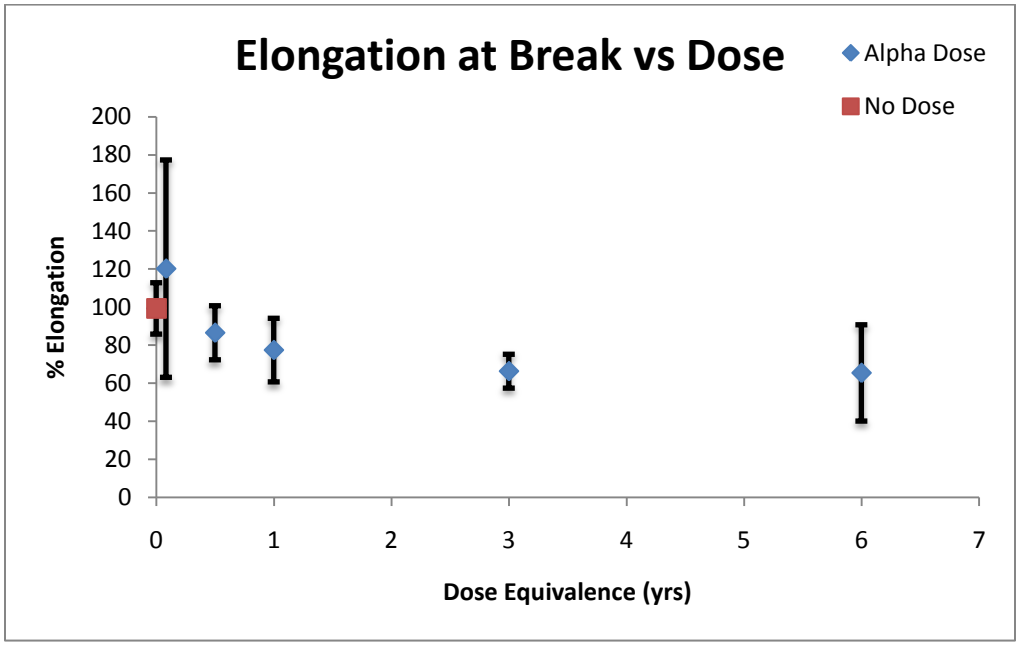

Figure 4.4: Percent Elongation at Break vs. Alpha Particle Dose. The relative elongation from initial shape at the point of material fracture for nylon 6,6 samples under irradiation is shown.

The percent elongation of the nylon 6,6 samples at fracture is plotted in Figure 4.4. While there appears to be some trending decrease in this mechanical property, the application of ANOVA statistics to the data shows the data sets become more indistinguishable for increasing dose. The maximum apparent change from the non-irradiated value occurs at an equivalent of 6 years of dose where the elongation is 34.14% less than the non-irradiated sample's elongation at

fracture. The average change in elongation over the range of doses was 24.67% from the initial elongation value.

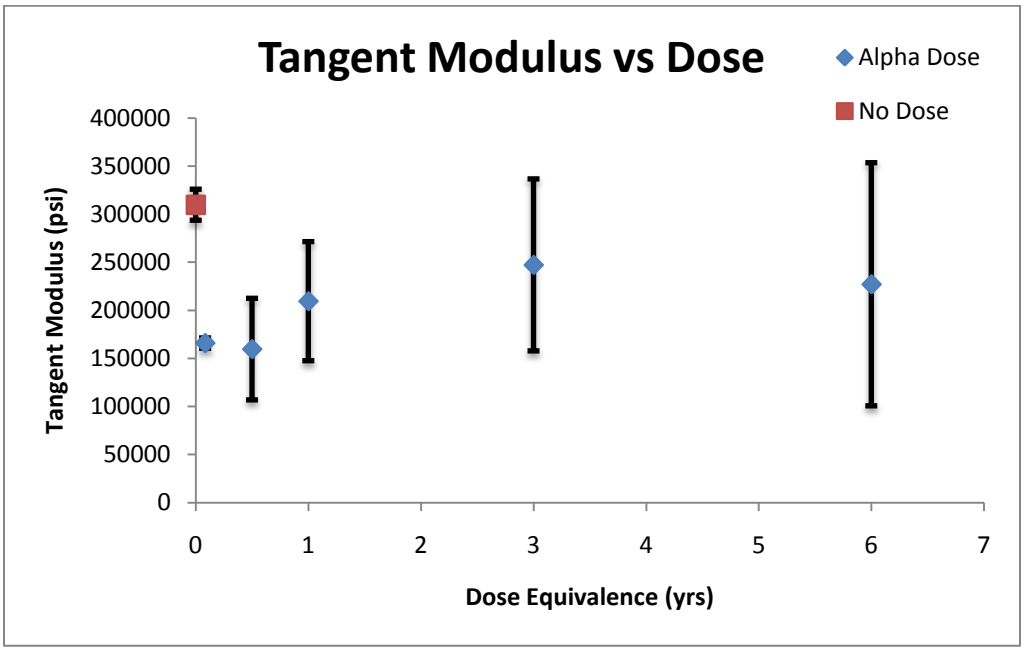

Figure 4.5: Tangent Modulus vs. Alpha Particle Dose. The tangent modulus from the stress-strain relationship for nylon 6,6 samples under irradiation is given.

The tangent modulus of the stress-strain relationship of nylon 6,6 material under alpha particle irradiation is shown in Figure 4.5. There appears to be a significant amount of change in this property with increasing dose at first glance. The initial advent of alpha particle irradiation results in a severe determent in the value of the tangent modulus compared to the initial value without irradiation. The maximum change in the modulus appears to occur at 6 months' worth of alpha particle dose where the modulus is decreased by 48.46% from the initial value. However, the measurements for the tangent modulus have the largest uncertainties of all the properties measured, especially at high dose. ANOVA

reveals that the irradiated sample sets are statistically distinguishable from the non-irradiated data set, but that they are not necessarily distinguishable from each other.

4.1.1 Color Indications of Alpha Irradiation

Given that the Fire Foe™ fire suppression system is expected to remain in constant operation within a glovebox for extended periods, it is useful to have some metric by which to determine the age of the system quickly from a cursory inspection. Figure 4.6 below shows several of the nylon 6,6 tensile samples through various stages of alpha particle irradiation by an ion beam.

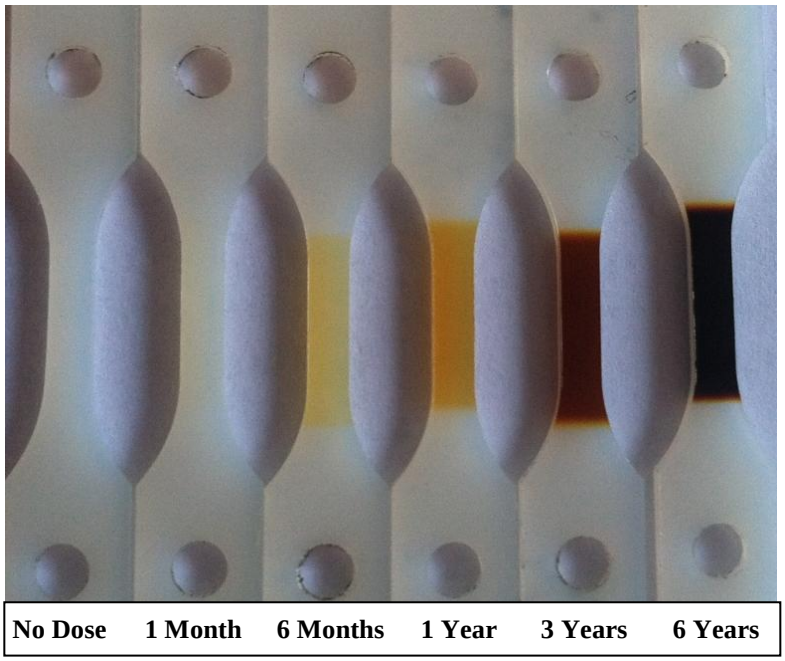

Figure 4.6: Discoloration in Nylon 6,6 after Alpha Irradiation. From left to right, the samples have received equivalent doses within the worst case glovebox of no dose, 1 month, 6 months, 1 year, 3 years, and 6 years.

Figure 4.6 shows the nylon 6,6 samples with increasing levels of dose applied. It seems that the higher the alpha particle radiation dose, then the darker the samples become. The alpha particles seem to mimic a burning effect on the outer surface of the effected region of the polymer. It is expected that this discoloration should be seen across the majority, if not the entirety, of the surface of a given Fire Foe™ fire suppression tube provided that the tube be kept constantly within a glovebox of similar radiative dose output to the worst case glovebox.

Another point of interest is the depth at which alpha particles are able to penetrate the nylon 6,6 material at various doses. The cross section of samples with doses equivalent to 6 months to 6 years is shown in Figure 4.7.

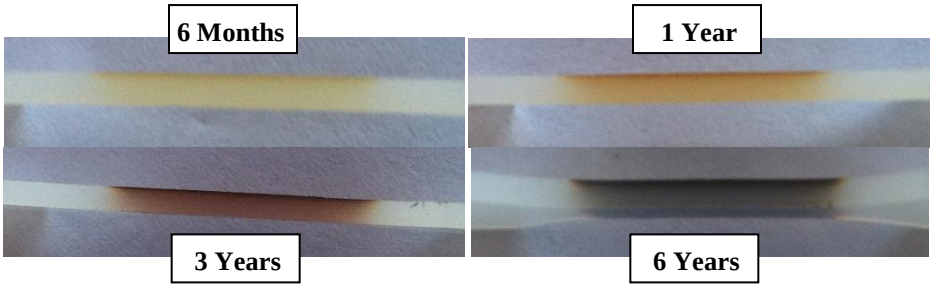

Figure 4.7: Nylon 6,6 Sample Cross Sections after Alpha Irradiation. Cross-sections of nylon 6,6 samples after the equivalent glovebox alpha irradiation of 6 months (upper left), 1 year (upper right), 3 years (lower left) and 6 years (lower right).

It seems to be the case that the majority of the alpha particles are deposited in the uppermost portions of a sample that are in direct contact with the radioactive source regardless of the amount of dose applied to the specimen. However, there does appear to be at least some level of deeper penetration into the rest of the material beyond this thin surface layer.

4.2 NEUTRON DAMAGE STUDIES

The second major source of radiation damage to materials inside a glovebox is due to neutrons. The neutron experiment began on 13 February 2012, when several samples were attached to the sample holder previously described in Chapter 3 and placed down the storage well along with the PuBe neutron source. The samples were affixed to the sample holder using Kapton tape due to the relative insensitivity of Kapton to radiation damage. The experiment sat undisturbed in the storage well until July 16th when the reactor bay at NETL became flooded. This resulted in the experiment being removed from the well until the water within the well could be removed. During this time, the experiment was placed over several other PuBe sources in separate, un-flooded storage well for approximately 28 hours. Following this period, the experiment was placed back within the original well. The experiment was ended after approximately 6 months of irradiation on 13 August 2012.

The mechanical testing results of the neutron damage experiment are given below in Table 4.5.

Table 4.5: Neutron Irradiation Experiment Results

Dose category	Tensile Strength		% Elongation		Tangent
	at yield	at break	at yield	at break	Modulus
Non-Irradiated Set	8704.8	7805.8	28.5	99.3	309,788.5
σ of Non-Irrad. Set	147.9	134.7	5.1	13.5	16,131.5
6 Month Dose	7059.3	7206.2	36.3	176.8	90,596.5
σ of 6 Month Dose	53.9	418.2	5.1	42.1	6,411.1

The data from Table 4.5 shows that after 6 months of neutron bombardment from a 5 Ci PuBe source, the mechanical properties of the nylon 6,6 material are altered greatly in some respects. The percent elongation at break appears to show a rather drastic upswing in its value prior to material failure. The large standard deviation in this result is due to the high degree of variability in pure polymers and the lack of homogeneity as discussed in Chapter 2.

Two of the mechanical properties stand out in terms of relative change from the non-irradiated sample set, namely the tensile strength of the material at yield and the tangent modulus. The strength at yield under neutron irradiation varies from the non-irradiated value by nearly 20%. This is over double the average variance from any of the samples sets under alpha particle irradiation. The tangent modulus saw a striking drop of upwards of 70% from the non-irradiated values. This value is also much less than any of tangent modulus measurements for any level of alpha particle dose.

The percent elongation at yield is slightly above the non-irradiated value, but the errors of both measurements overlap so the statistical significance suggests a null difference. The tensile strength at break was reduced by less than 10% from the non-irradiated value and is comparable to the values obtained after level of alpha particle dose. All neutron irradiated data sets were determined to be statistically distinguishable from the non-irradiated data past the 95% confidence level using ANOVA techniques.

4.2.1 Neutron Specimen Discoloration

The level discoloration of the samples due to neutron dose is also of interest. Figure 3.8 below shows a neutron irradiated specimen of nylon 6,6 compared to a non-irradiated sample and a 6 month alpha dose sample.

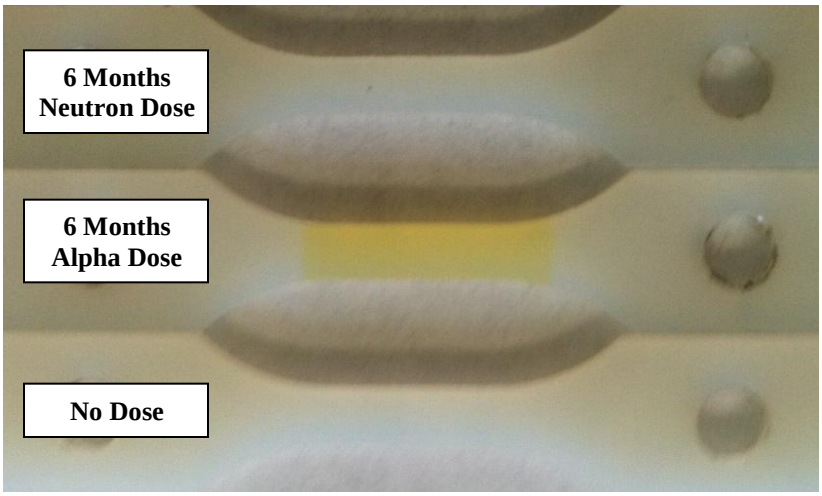

Figure 4.8: Discoloration of Nylon 6,6 after Neutron Irradiation. The top specimen is nylon 6,6 after 6 months of irradiation by the 5 Ci PuBe source at NETL. The center specimen is nylon after 6 months of equivalent dose in a glovebox from an ion beam, and the bottom specimen is non-irradiated.

It is readily apparent from the above figure that neutron damage, at least from 6 months' worth accumulated near a 5 Ci PuBe source, does not leave significant visual traces on nylon 6,6 material. This also indicates that the neutrons are able to completely penetrate through the depth of the nylon casing present in the Fire Foe™ system.

The samples were also measured for activity immediately after irradiation had ended. There was no discernible activity present in any specimen above the

level of background present in the laboratory. This indicates that the nylon material was not, in fact, activated by the high flux of neutrons.

Chapter 5: Discussion of Results

The data collected on how the nylon material changes under irradiation is important for a variety of reasons. The most essential reason is being able to quantify the changes in the material of the Fire Foe™ system over a period of time spent in a glovebox. The Fire Foe™ systems are rated to last upwards of 6 years if kept under normal conditions with non-corrosive environments. However, since this is not possible for the system in use within gloveboxes, it becomes important to know if the mean lifetime of these systems is expected to be effected by the glovebox conditions.

5.1 ALPHA PARTICLE DAMAGE STUDIES

The results obtained from the mechanical tensile testing of the samples irradiated in the alpha particle ion beam are very useful in understanding how the material should be expected to evolve over the course of many years as it is being irradiated within a glovebox. The first thing that should be pointed out is the change in the tensile strength both at the yield and fracture points and the percent elongation at the yield point all vary from the non-irradiated samples by less than 8% on average across for doses due to alpha particles. This level of change is not likely to result in a drastic compromise of the material over its lifetime in a glovebox. That is to say that the effect of alpha particle irradiation incident on the nylon 6,6 casing is not expected to have a greatly detrimental effect on the mean lifetime of the Fire Foe™ systems within gloveboxes.

Another interesting result is the relative decrease in the percent elongation at break with increasing dose. This relative differential is not evident in the percent elongation at yield data. This suggests that Fire Foe™ systems that have been in place in plutonium gloveboxes longer will experience a faster transformation between the points of yield and fracture. The level of plastic deformation that the nylon 6,6 casing is expected to experience prior fracturing and as a result of alpha particle dose should be reduced for higher levels of dose. This is to say that the nylon 6,6 should expand less before fracturing with more time spent under alpha particle irradiation in a glovebox. It could also be the case that in the event of a fire resulting in ultimate failure and rupture of the Fire Foe™ system that the nylon will fracture slightly more quickly after having been irradiated for longer periods of time in a glovebox.

The changes to the tangent modulus as a function of dose are also quite striking. This was the material property that changed the most with alpha dose relative to the initial non-irradiated sample sets. There appears to be upwards of 35% difference on average between the alpha irradiated samples and the non-irradiated sample set, however, there is a considerable overlap of the errors in these measurements making definite conclusions difficult. Since the tangent modulus is the slope of the stress-strain curve at a given point for a material, then it follows that for two samples with differing moduli that the amount of stress required which results in similar levels of strain will be greater for the sample with the greater modulus. Beyond the yield point the tangent modulus also provides insight into the softening of the material being tested. From the data, it

appears that alpha particle irradiation causes a significant degree of hardening within the nylon material. The errors on the measurements of this tensile property are very high for dose equivalences corresponding to 1, 3 and 6 years in a glovebox. In the cases of the 3 and 6 year doses, these high errors place the ranges of the tangent moduli well within the initial value of the non-irradiated sample set and as such are not satisfactorily statistically significant results.

The discoloration of the samples after irradiation is striking and may prove to be a useful feature in determining relative ages of the Fire Foe™ systems in place within gloveboxes using only cursory examination. The discoloration of the samples appears to grow progressively darker and browner with increasing alpha particle dose. This darkening of the sample is indicative of progression of degradation of the nylon material under increasing dose, and serves as a visual indicator of the breakdown of polymer chains within the nylon, oxidation of the polymer, or increases in cross-linking within the polymer matrix.

From discussions with Michael Cournoyer, the degradation of the polymer is said to commence through the removal of a hydrogen atom from the polymer chain by some ionized particle, either an alpha particle or else some knock-off atom resulting from previous interactions with an alpha particle. The removal of a hydrogen atom begins a large chain reaction within the polymer resulting in further loss or displacement of hydrogen. It is believed that the initial hydrogen removal reaction occurs within the N-vicinal methylene group which is adjacent to the -NH- group within the polymer chain. The degradation reaction can also begin within the amide group in the nylon. The ultimate result of this is the

formation of colored molecules within the structure of the nylon 6,6 sample followed by a chain of scissions along the polymer. As this reaction advances, the chain-scission reactions have a larger effect on the whole of the polymer matrix and detrimental effects on the mechanical properties of the nylon are asserted.

The discoloration of a particular sample at any given dose is noted to be segregated through depth into the sample. This is to say that the majority of the discoloration is confined to a thin layer near the surface of irradiation for a given sample. This is not unexpected and conforms to the prediction of the MCNPX model that majority of deposition of alpha particles into the nylon 6,6 samples will be very shallow. The surface deposition of alpha particles also means that the particles are unlikely to penetrate deep enough into the tube of the Fire Foe™ system such that the sodium bicarbonate extinguishment fill within the tube will be affected or else chemically altered by the radiation.

It was also noted during the course of the alpha irradiation in the ion beam that the nylon 6,6 specimens scintillated with visible light emissions. This behavior is not entirely unexpected for a material composed of low-Z material. The intensity of the light generated through scintillation of the material was observed to be low enough that it was visible only under pitch darkness with a close-up camera view. This scintillation behavior serves as a visual conformation of ionization events caused by alpha particle irradiation.

5.2 NEUTRON DAMAGE STUDIES

The results of the neutron damage study show the effects of neutron damage on the nylon 6,6 material is far more drastic than for any level of alpha particle dose. The tensile strength at yield was seen to decrease by nearly 20%, over twice what was seen with alpha particle irradiation at any dose level. However, the value for the tensile strength at break was comparable to the values seen in alpha irradiated samples and varied from the non-irradiated sample set by less than 10%. It is not clear if the decrease in the tensile strength at yield is significant enough to seriously affect or reduce the lifetime of a Fire Foe™ tube system placed within a plutonium glovebox.

The percent elongation at yield of the samples under neutron irradiation appears to shift slightly upward, but this is not statistically significant due to the overlap in the errors of the neutron sample set and the non-irradiated sample set. However, the elongation at break appears to be significantly increased with respect to the non-irradiated sample set. This means that the nylon material will likely expand much more before fracturing during an event such as a fire. This result is in contrast to the results from the alpha irradiation experiment which suggested a slight decreasing trend in the elongation at break with higher dose.

The tangent modulus of the nylon 6,6 was noted to the most effected mechanical property under neutron irradiation. This property suffered a severe decrease from the non-irradiated sample set of nearly 70%. This suggests that neutron damage causes a significant degree in the hardening of the nylon material.

This difference is much more pronounced than in the case of any level of alpha particle dose.

One possible explanation for the significant differences in mechanical properties between neutron and alpha particle irradiated samples lies within the nature of the damaging particles themselves. Alpha particles are not highly penetrative through nylon or any other material, as has been seen in the body of this work. This means that majority of the damage from alpha particles is confined to a small portion of the sample specimens. Neutrons are very highly penetrative and as such are likely to have a more evenly distributed level of damage through the nylon specimens. This is similar to demolishing a high rise building. It is far more efficient to damage the support structures of the building dispersed throughout its interior using explosives than to use a wrecking ball on only one side. Here, of course, the support structures are the intermolecular bonds within the polymer matrix.

The lack of apparent discoloration in the nylon 6,6 samples following neutron bombardment supports previous assertions about the interaction of neutrons and nylon. For one, neutrons must be very penetrative through the nylon material due to the lack of obvious scattering along the side of each sample facing the PuBe source and as seen in the alpha irradiated samples in the ion beam. This penetration of neutrons could potentially lead to neutron interactions with the sodium bicarbonate and inert gas compounds contained within the Fire Foe™ tube. Another insight about this lack of discoloration is that only alpha particle damage and discoloration should be an indicator as to the age of a particular Fire

Foe™ system within a given glovebox. However, it is unclear if higher doses at longer irradiation times from a neutron source would cause any discoloration to appear within the sample.

5.3 FUTURE AREAS OF FOCUS

The experiments conducted during the course of this project have focused solely on radiation damage from neutrons and alpha particles incident on the nylon 6,6 casing of Fire Foe™ systems within gloveboxes. No considerations were made with regard to how these systems behave in gloveboxes containing experiments using acids or other corrosive substances. It is entirely within reason to assume that corrosive elements will have caustic reactions with the nylon 6,6 casing material of the Fire Foe™ systems. However, how detrimental these corrosive elements would be to nylon 6,6 material properties is unknown especially in the presence of a radiation field consisting of alpha particles and neutrons.

Elevated heat levels that may result from experiments using a heating source or else from large enough radioactive sources that may be thermally radiative are also unaccounted for in the body of this work. Such heat sources may cause additional softening in the nylon 6,6 casing material leading to increased damage from radiological sources, thermal expansion of the material, and possible increased permeability of radiation that might adversely affect the sodium bicarbonate filling. These thermal sources may cause an overall decrease in the effective lifetime of a Fire Foe™ system within a particular glovebox.

Gamma ray radiation is another common form of glovebox radiation. However, the effect of gamma rays on nylon 6,6 specimens was not explicitly examined during the course of experimentation. Gamma rays are known to have a strengthening effect on other types of nylon and other polymers through the processes cross-linking of molecular chains within polymer matrices. Gamma rays are also very penetrative through low density material such as nylon. This penetration is likely to result in gamma ray interaction with the internal sodium bicarbonate material and result in some level of chemical change within the fill.

Likewise, it is unknown to what extent neutrons may alter the internal filling of the Fire Foe™ system. Experiments may need to be conducted using high dose neutron sources on this filling material followed by chemical analysis. It may also be possible to simulate the effects of neutron irradiation on this material through the use of computer modeling with codes like MCNP.

In experiments with multiple sources of potential material damage, including caustic, thermal, and radiative sources, it is likely that these sources would act in concert to effect change to the nylon 6,6 casing material. However, it is not possible to explicitly state the extent to which the nylon 6,6 material would be effected or which process should dominate the changes to the material properties of the nylon 6,6 casing and the underlying sodium bicarbonate filling. Ultimately, further studies will be necessary to determine how the mean lifetime of the Fire Foe™ system is altered when placed in gloveboxes with multiple potential sources of material damage.

Chapter 6: Conclusions

Plutonium gloveboxes house a significant quantity of special nuclear material critical to national security and industrial applications. The gloveboxes themselves serve as a barrier between the experiments and the workers conducting them. Historically, plutonium gloveboxes have been prone to catch fire easily, often resulting in disastrous damage to facilities and the release of hazardous nuclear material to the environment. Over the decades since nuclear gloveboxes have been implemented, safety measures designed to mitigate the potential for disaster have been added progressively. The latest such safety measure is the addition of the Fire Foe™ fire suppression system which is capable of quickly and independently extinguishing fires within gloveboxes.

This project has placed the casing material of the Fire Foe™ system, namely the polymer nylon 6,6, under extensive review. The effects of increasing levels of alpha particle irradiation on specimens of the nylon 6,6 material were shown to be slightly detrimental to the tensile strength of the material. The percent of elongation of the material at yield was determined to not vary much with increasing alpha particle dose. However, the percent elongation at the point of fracture of the specimens appeared to decrease as much as 34% at the highest levels of alpha particle dose, but this result is mired by statistical uncertainty. The tangent modulus mechanical property appeared to decrease by upwards of 48% for alpha particle doses simulating up to 6 months within a plutonium glovebox, but again the statistical significance of this result is hindered by overlapping

errors. However, this decrease in the tangent modulus decreased sharply for very high doses out to 6 years in a glovebox.

The alpha particle irradiation was conducted using an alpha particle ion beam located at the Material Science Laboratory on the Los Alamos campus. It was determined early on in the project that traditional alpha particle point sources, such as actinides like ^{244}Cm, would be unsuitable for the needs of the experiment. This is because the point sources currently commercially available are of such low activity that the irradiation times involved in using them would be very excessive. The alpha particle ion beam is capable of delivering doses to samples comparable to 6 years in a extremely high dose plutonium glovebox in only approximately 3 hours.

The neutron damage study was conducted using a 5 Ci PuBe source located at the Nuclear Engineering Teaching Laboratory on the University of Texas Pickle Research Campus. The nylon 6,6 samples were irradiated for 6 months within a closed container lowered down into a storage well in the bay of the facility's TRIGA research reactor.

The results of the neutron damage study show that the effect of neutron irradiation on nylon is more pronounced than alpha irradiation in several aspects. The tensile strength at break was noted to be decreased by nearly 20%, which was more than twice the level of change seen in any level of alpha particle dose. The tensile strength at break and elongation at yield was not noted to be significantly different from the results obtained for the alpha irradiation experiment. However, the tensile strength at break was determined increase rather drastically for the

neutron irradiated samples, and the tangent modulus was also noted to be significantly decreased by as much as 70% from the non-irradiated sample set values. There was no detectable discoloration in the samples irradiated by the neutron source.

It would seem that neutrons have a more profound effect on the mechanical properties of the nylon 6,6 material than alpha particles. However, the alpha particles offer a more pronounced visual cue to radiation damage through discoloration of the nylon.

Appendix A: Alpha Particle Source Data

The following is a table of the alpha particle data from the source previously specified. This data was used in the determination of dose from Sources 4C and MNCPX.

Table A: Alpha Particle Source Data

Alpha Energy (MeV)	Alpha Particles per sec per cm^2		Alpha Energy (MeV)	Alpha Particles per sec per cm^2		Alpha Energy (MeV)	Alpha Particles per sec per cm^2
0.033	2.18E+06		1.918	1.53E+05		3.803	2.16E+05
0.098	3.09E+05		1.983	1.56E+05		3.868	2.18E+05
0.163	2.25E+05		2.048	1.58E+05		3.933	2.19E+05
0.228	1.87E+05		2.113	1.61E+05		3.998	2.21E+05
0.293	1.64E+05		2.178	1.63E+05		4.063	2.23E+05
0.358	1.50E+05		2.243	1.65E+05		4.128	2.25E+05
0.423	1.40E+05		2.308	1.68E+05		4.193	2.27E+05
0.488	1.33E+05		2.373	1.70E+05		4.258	2.28E+05
0.553	1.28E+05		2.438	1.73E+05		4.323	2.30E+05
0.618	1.25E+05		2.503	1.75E+05		4.388	2.32E+05
0.683	1.23E+05		2.568	1.77E+05		4.453	2.33E+05
0.748	1.22E+05		2.633	1.79E+05		4.518	2.35E+05
0.813	1.21E+05		2.698	1.82E+05		4.583	2.37E+05
0.878	1.22E+05		2.763	1.84E+05		4.648	2.38E+05
0.943	1.22E+05		2.828	1.86E+05		4.713	2.40E+05
1.008	1.23E+05		2.893	1.88E+05		4.778	2.42E+05
1.073	1.25E+05		2.958	1.90E+05		4.843	2.43E+05
1.138	1.26E+05		3.023	1.92E+05		4.908	2.45E+05
1.203	1.28E+05		3.088	1.94E+05		4.973	2.47E+05
1.268	1.30E+05		3.153	1.96E+05		5.038	2.48E+05
1.333	1.32E+05		3.218	1.98E+05		5.103	2.40E+05
1.398	1.34E+05		3.283	2.00E+05		5.168	1.08E+05
1.463	1.36E+05		3.348	2.02E+05		5.233	5.24E+04
1.528	1.39E+05		3.413	2.04E+05		5.298	5.27E+04
1.593	1.41E+05		3.478	2.06E+05		5.363	5.30E+04
1.658	1.43E+05		3.543	2.08E+05		5.428	5.20E+04
1.723	1.46E+05		3.608	2.10E+05		5.493	2.17E+04
1.788	1.48E+05		3.673	2.12E+05		5.558	1.19E+01
1.853	1.51E+05		3.738	2.14E+05		Sum	1.69E+7

Appendix B: Full Tensile Testing Data

The following tables are the results from tensile testing on nylon 6,6 specimens done according to ASTM D638 and reported by Polyhedron Laboratories in Houston, TX.

Table B.1: Non-Irradiated Tensile Testing Data

	Tensile Strength		% Elongation		Tangent Modulus (psi)
	at yield (psi)	at break (psi)	at yield	at break	
	8627.4	7838.8	35.7	101.7	301,490.5
	8894.1	7684.1	29.3	82.3	293,910.0
	8816.3	7978.5	21.3	92.0	329,513.1
	8528.9	7871.9	27.7	118.7	299,346.6
	8657.2	7655.8	28.7	101.7	324,682.1
Average	8704.8	7805.8	28.5	99.3	309,788.5
Error	147.9	134.7	5.1	13.5	16,131.5

Table B.2: 1 Month Alpha Dose Equivalent Tensile Data

	Tensile Strength		% Elongation		Tangent Modulus (psi)
	at yield (psi)	at break (psi)	at yield	at break	
	8264.8	7031.7	30.0	85.3	248,992.7
	8195.9	7343.9	27.7	63.3	188,027.1
	7725.0	7372.5	32.3	136.0	120,529.1
	7855.1	7809.6	32.7	210.3	143,716.0
	7718.5	7020.0	33.0	106.0	128,279.4
Average	7951.9	7315.6	31.1	120.2	165,908.9
Error	261.1	322.5	2.3	57.1	5,391.6

Table B.3: 6 Month Alpha Dose Equivalent Tensile Data

	Tensile Strength		% Elongation		Tangent Modulus (psi)
	at yield (psi)	at break (psi)	at yield	at break	
	7680.5	6792.1	38.0	104.3	114,004.3
	7764.0	6861.3	30.7	99.3	129,528.3
	7969.6	7048.6	28.7	78.7	247,148.3
	7994.8	7251.6	36.3	77.0	138,864.8
	8411.8	7610.6	38.3	73.3	168,708.2
Average	7964.2	7112.9	34.4	86.5	159,650.8
Error	283.7	330.6	4.4	14.2	52,822.5

Table B.4: 1 Year Alpha Dose Equivalent Tensile Data

	Tensile Strength		% Elongation		Tangent Modulus (psi)
	at yield (psi)	at break (psi)	at yield	at break	
	8117.4	6956.6	36.7	104.3	137,662.3
	8032.0	6912.1	25.0	79.0	284,395.9
	8137.7	7358.7	35.3	74.7	187,287.6
	8082.7	7122.8	21.7	59.3	263,126.3
	7927.7	7178.1	28.3	69.7	174,900.9
Average	8059.5	7105.7	29.4	77.4	209,474.6
Error	83.3	179.7	6.5	16.7	61,919.9

Table B.5: 3 Year Alpha Dose Equivalent Tensile Data

	Tensile Strength		% Elongation		Tangent Modulus (psi)
	at yield (psi)	at break (psi)	at yield	at break	
	8051.4	7357.7	26.0	61.7	353,311.5
	8270.0	7435.0	28.7	61.0	185,005.4
	8327.7	7409.0	31.3	78.3	197,975.9
	8020.3	7412.9	32.0	57.7	165,001.0
	8245.0	7479.5	29.7	73.0	334,828.2
Average	8182.9	7418.8	29.5	66.3	247,224.4
Error	138.0	44.2	2.4	8.9	89,423.4

Table B.6: 6 Year Alpha Dose Equivalent Tensile Data

	Tensile Strength		% Elongation		Tangent Modulus (psi)
	at yield (psi)	at break (psi)	at yield	at break	
	8212.1	6904.1	21.0	64.7	430,299.0
	8138.8	7534.6	29.0	60.0	163,023.3
	8092.0	7458.1	24.7	36.3	269,610.5
	8261.5	6939.5	33.3	106.0	127,476.0
	8167.3	7091.9	29.7	60.0	144,628.3
Average	8174.3	7091.9	27.5	65.4	227,007.4
Error	65.4	389.9	4.8	25.3	126,421.2

Table B.7: Neutron Experiment Tensile Data

	Tensile Strength		% Elongation		Tangent Modulus (psi)
	at yield (psi)	at break (psi)	at yield	at break	
	6981.0	6704.6	37.7	143.7	92,529.1
	7050.5	7240.4	29.0	149.3	99,516.8
	7088.1	6998.6	38.7	198.0	92,193.5
	7126.4	7840.3	42.3	241.3	83,646.6
	7050.5	7247.3	33.7	151.7	85,096.3
Average	7059.3	7206.2	36.3	176.8	90,596.5
Error	53.9	418.2	5.1	42.1	6,411.1

Appendix C: ANOVA (Single Factor) Statistics of Tensile Data

Select ANOVA results for specified tensile properties and data sets are given.

Table C.1: Yield Strength No Dose/1 Month Alpha Analysis

Groups	*Count*	*Sum*	*Average*	*Variance*
No dose	5	43523.9	8704.78	21866.02
1 Month Alpha	5	39759.3	7951.86	68192.95

ANOVA

Source of Variation	*SS*	*df*	*MS*	*F*	*P-value*	*F crit*
Between Groups	1417221	1	1417221	31.47319	0.000504	5.317655
Within Groups	360235.9	8	45029.48			
Total	1777457	9				

Table C.2: Yield Strength 1 Month Alpha/6 Month Alpha Analysis

Groups	*Count*	*Sum*	*Average*	*Variance*
1 Month Alpha	5	39759.3	7951.86	68192.95
6 Month Alpha	5	39820.7	7964.14	80469.25

ANOVA

Source of Variation	*SS*	*df*	*MS*	*F*	*P-value*	*F crit*
Between Groups	376.996	1	376.996	0.005072	0.944973	5.317655
Within Groups	594648.8	8	74331.1			
Total	595025.8	9				

Table C.3: Yield Strength 1 Year Alpha/6 Year Alpha Analysis

Groups	*Count*	*Sum*	*Average*	*Variance*
1 Year Alpha	5	40297.5	8059.5	7033.345
6 Year Alpha	5	40871.7	8174.34	4278.803

ANOVA

Source of Variation	*SS*	*df*	*MS*	*F*	*P-value*	*F crit*
Between Groups	32970.56	1	32970.56	5.829231	0.042219	5.317655
Within Groups	45248.59	8	5656.074			
Total	78219.16	9				

Table C.4: Yield Strength No Dose/Neutron Dose Analysis

Groups	*Count*	*Sum*	*Average*	*Variance*
No dose	5	43523.9	8704.78	21866.02
Neutron Dose	5	35296.5	7059.3	2904.405

ANOVA

Source of Variation	*SS*	*df*	*MS*	*F*	*P-value*	*F crit*
Between Groups	6769011	1	6769011	546.5398	1.19E-08	5.317655
Within Groups	99081.69	8	12385.21			
Total	6868093	9				

Table C.5: Break Strength No Dose/1 Month Alpha Analysis

Groups	*Count*	*Sum*	*Average*	*Variance*
No dose	5	39029.1	7805.82	18148.6
1 Month Alpha	5	36577.7	7315.54	104013.3

ANOVA

Source of Variation	*SS*	*df*	*MS*	*F*	*P-value*	*F crit*
Between Groups	600936.2	1	600936.2	9.83836	0.013876	5.317655
Within Groups	488647.4	8	61080.93			
Total	1089584	9				

Table C.6: Break Strength No Dose/Neutron Dose Analysis

Groups	*Count*	*Sum*	*Average*	*Variance*
No dose	5	39029.1	7805.82	18148.6
Neutron Dose	5	36031.2	7206.24	174910.5

ANOVA

Source of Variation	*SS*	*df*	*MS*	*F*	*P-value*	*F crit*
Between Groups	898740.4	1	898740.4	9.310522	0.015789	5.317655
Within Groups	772236.4	8	96529.54			
Total	1670977	9				

Table C.7: Break Strength 6 Month Alpha/3 Year Alpha Analysis

Groups	*Count*	*Sum*	*Average*	*Variance*
6 Month Alpha	5	35564.2	7112.84	109323.2
3 Year Alpha	5	37094.1	7418.82	1952.747

ANOVA

Source of Variation	*SS*	*df*	*MS*	*F*	*P-value*	*F crit*
Between Groups	234059.4	1	234059.4	4.20683	0.074386	5.317655
Within Groups	445103.6	8	55637.96			
Total	679163	9				

Table C.8: Yield Elongation No Dose/1 Month Alpha Analysis

Groups	*Count*	*Sum*	*Average*	*Variance*
No dose	5	142.7	28.54	26.248
1 Month Alpha	5	155.7	31.14	5.093

ANOVA

Source of Variation	*SS*	*df*	*MS*	*F*	*P-value*	*F crit*
Between Groups	16.9	1	16.9	1.07846	0.329409	5.317655
Within Groups	125.364	8	15.6705			
Total	142.264	9				

Table C.9: Yield Elongation 3 Year Alpha/6 Year Alpha Analysis

Groups	*Count*	*Sum*	*Average*	*Variance*
3 Year Alpha	5	147.7	29.54	5.603
6 Year Alpha	5	137.7	27.54	22.703

ANOVA

Source of Variation	*SS*	*df*	*MS*	*F*	*P-value*	*F crit*
Between Groups	10	1	10	0.706564	0.424995	5.317655
Within Groups	113.224	8	14.153			
Total	123.224	9				

Table C.10: Yield Elongation No Dose/Neutron Dose Analysis

Groups	*Count*	*Sum*	*Average*	*Variance*
No dose	5	142.7	28.54	26.248
Neutron Dose	5	181.4	36.28	25.942

ANOVA

Source of Variation	*SS*	*df*	*MS*	*F*	*P-value*	*F crit*
Between Groups	149.769	1	149.769	5.739375	0.043467	5.317655
Within Groups	208.76	8	26.095			
Total	358.529	9				

Table C.11: Break Elongation No Dose/1 Year Alpha Analysis

Groups	*Count*	*Sum*	*Average*	*Variance*
No dose	5	496.4	99.28	182.542
1 Year Alpha	5	387	77.4	280.09

ANOVA

Source of Variation	*SS*	*df*	*MS*	*F*	*P-value*	*F crit*
Between Groups	1196.836	1	1196.836	5.17403	0.052508	5.317655
Within Groups	1850.528	8	231.316			
Total	3047.364	9				

Table C.12: Break Elongation 1 Year Alpha/3 Year Alpha Analysis

Groups	*Count*	*Sum*	*Average*	*Variance*
1 Year Alpha	5	387	77.4	280.09
3 Year Alpha	5	331.7	66.34	78.023

ANOVA

Source of Variation	*SS*	*df*	*MS*	*F*	*P-value*	*F crit*
Between Groups	305.809	1	305.809	1.707891	0.227572	5.317655
Within Groups	1432.452	8	179.0565			
Total	1738.261	9				

Table C.13: Break Elongation No Dose/Neutron Dose Analysis

Groups	*Count*	*Sum*	*Average*	*Variance*
No dose	5	496.4	99.28	182.542
Neutron Dose	5	884	176.8	1772.89

ANOVA

Source of Variation	*SS*	*df*	*MS*	*F*	*P-value*	*F crit*
Between Groups	15023.38	1	15023.38	15.36579	0.004419	5.317655
Within Groups	7821.728	8	977.716			
Total	22845.1	9				

Table C.14: Tangent Modulus No Dose/1 Year Alpha Analysis

Groups	*Count*	*Sum*	*Average*	*Variance*
No dose	5	1.55E+06	3.10E+05	2.60E+08
1 Year Alpha	5	1.05E+06	2.09E+05	3.83E+09

ANOVA

Source of Variation	*SS*	*df*	*MS*	*F*	*P-value*	*F crit*
Between Groups	2.52E+10	1	2.52E+10	12.28887	0.008014	5.317655
Within Groups	1.64E+10	8	2.05E+09			
Total	4.15E+10	9				

Table C.15: Tangent Modulus 6 Month Alpha/6 Year Alpha Analysis

Groups	*Count*	*Sum*	*Average*	*Variance*
6 Month Alpha	5	798253.9	159650.8	2.79E+09
6 Year Alpha	5	1135037	227007.4	1.6E+10

ANOVA

Source of Variation	*SS*	*df*	*MS*	*F*	*P-value*	*F crit*
Between Groups	1.13E+10	1	1.13E+10	1.208392	0.303628	5.317655
Within Groups	7.51E+10	8	9.39E+09			
Total	8.64E+10	9				

Table C.16: Tangent Modulus No Dose/Neutron Dose Analysis

Groups	*Count*	*Sum*	*Average*	*Variance*
No dose	5	1548942	309788.5	2.6E+08
Neutron	5	452982.3	90596.46	41102603

ANOVA

Source of Variation	*SS*	*df*	*MS*	*F*	*P-value*	*F crit*
Between Groups	1.2E+11	1	1.2E+11	797.2269	2.67E-09	5.317655
Within Groups	1.21E+09	8	1.51E+08			
Total	1.21E+11	9				

References

ASTM, "Standard Test Method for Tensile Properties of Plastics," American Society for Testing and Materials (ASTM) standard D638-10.

ASTM, "Standard Test Method for Determining Thermal Neutron Reaction and Fluence Rates by Radioactivation Techniques," American Society for Testing and Materials (ASTM) standard E262-03.

Bhattacharya, A., "Radiation and Industrial Polymers," *Prog. Polym. Sci.*, 25, pp. 371-401, 2000.

Buffer, P. *Rocky Flats Site History*. Department of Energy. DOE.gov, Retrieved 25 April 2012.

Casey, J., 2004, *Minimizing Glovebox Glove Breeches in Plutonium Handling Facilities at Los Alamos National Laboratory*, Thesis, MS, University of Texas, USA, 2004.

Chapiro, A., "General consideration of the radiation chemistry of polymers," *Nuclear Instruments and Methods in Physics Research B*, 105, pp. 5-7, 1995.

Chen, *et al.*, "Effect of γ-Radiation of the Property of Polypropylene/Nylon-6 Blends," *Advanced Materials Research*, 320, pp. 69-74, 2011.

Corneliussen, R., "Nylon 66 Molding Compound Properties", maropolymeronline.com, Maro Polymer Links, 2002, Retrieved 25 November, 2011.

Cournoyer, Balkey, Casey, Taylor, Stimmel, and Zaelke, "Minimizing Glovebox Glove Breaches," LA-UR-04-6339, Los Alamos National Laboratory, 2004.

Cournoyer, Wilson, Maestas, and Schreiber, "Minimizing Glovebox Glove Breaches, Part III: Deriving Service Lifetimes," Los Alamos National Laboratory, 2006.

Cournoyer and Schreiber, "Using Pressure Decay Methodology to Detect Glovebox Failures," *American Glovebox Society Enclosure*, 21, pp. 6-14, 2008.

Davenas, J., *et al.*, "Ion beam induced conversion of PVC into conducting polyene," *Synthetic Metals*, 69, pp. 583-584, 1995.

Deeley, C. W., Woodward, and Sauer, "Effect of Irradiation on Dynamic Modeling Properties of 6-6 Nylon," *Journal of Applied Physics*, 28 (10), pp. 1124-1130, 1957.

DOE Fundamentals Handbook: Materials Science, U.S. Department of Energy, DOE-HDBK-1017/1-93, 1993.

Ellison, *et al.*, "High Energy Radiation Effects on Ultimate-Mechanical Properties and Fractography of Nylon-6 Fibers," *Journal of Material Science*, 19 (1), pp. 82-98, 1984.

Elving, P.J., and Kolthoff, I.M., "Neutron Activation Analysis," Part 1, John Wiley & Sons, 1972.

ENDF Data, Electronic Data Files for neutron cross-sections data maintained by the National Nuclear Data Center (NNDC), Brookhaven National Laboratory (BNL), www.nndc.bnl.gov, Retrieved 30 July 2012.

Fadel *et al.*, "Possible control of the mechanical properties of nylon-6, dralon, and polyester polymers by neutron irradiation," Polymer Degradation and Stability, 23 (3), pp. 209-216, 1989.

Griffen, M., *Evaluation of Hypalon and Polyurethane for Use in Plutonium Glovebox Environments*, Thesis, MSE, University of Texas, USA, 2006.

Hourston, D. J., and Brysdon, J. A., "Degradation of Plastics and Polymers," *Elsevier B. V.*, 2010.

"Hypalon Technical Data Sheet", lancopaints.com. Lanco., 2005, Retrieved 25 November, 2011.

James, A., and Coutlee, S., "Polymer Synthesis Lab," Wellesley College, Department of Chemistry, http://www.wellesley.edu/Chemistry/, 2006, Retrieved 23 July 2012.

KAERI, Korea Atomic Energy Research Institute. atom.kaeri.re.kr/index.html, 2000, Retrieved 5 July 2012.

LaMarsh, J. R. and Baratta, A. J., *Introduction to Nuclear Engineering*, 3rd Edition, Prentice Hall, 2001.

Leonard, M. T. and McClure, P. R., "Mechanistic Analysis of Glovebox Fire Propagation," LA-UR-99-2677, Los Alamos National Laboratory, 1999.

Linggawati, A., Mohammad, A., and Ghazali, Z., "Effect of electron beam irradiation on morphology and sieving characteristics of nylon-66 membranes," *European Polymer Journal*, 45, pp. 2797-2804, 2009.

Murphy, *et al.*, "Volatile evolution from polymer materials induced by irradiation with He++ ions and comparative pyrolysis experiments," *Nuclear Instruments and Methods in Physics Research B*, 215, pp. 423-435, 2004.

Olivares, *et al.*, "FT-Raman analysis of the effects of γ-radiation on Nylon 6-12 filaments," *Polymer Bulletin*, 37, pp. 221-228, 1996.

Pelowitz, D. B., "MCNPX™ User's Manual," LA-CP-07-1473, Los Alamos National Laboratory, 2008.

"Physical, Nuclear, and Chemical Properties of Plutonium," http://www.ieer.org/fctsheet/pu-props.html, Institute for Energy and Environmental Research, 2008, Retrieved 24 November 2011.

Quick Fire, "Fire Foe Products," http://www.quick-fire.com/products-01.asp, Quick Fire-Fire Suppression Technology, 2011, Retrieved 27 November 2011.

Shultis, J. K., and Faw, R. E., "Radiation Shielding," American Nuclear Society, 2000.

Trossarelli, L., "The History of Nylon," Club Alpino Italiano, Centro Studi Materiali e Tecniche, www.caimateriali.org/index, 2010, Retrieved 8 August 2012

Wang, Y. Q., "Ion Beam Materials Laboratory," LALP-06-036, Los Alamos National Laboratory, 2006.

Was, G. S., *Fundamentals of Radiation Materials Science: Metals and Alloys*, Springer Science, 2007.

Wilson, W.B, *et al.*, "SOURCES 4C: A Code for Calculating (alpha, n), Spontaneous Fission, and Delayed Neutron Sources and Spectra," LA-UR-02-1839, Los Alamos National Laboratory, 2002.

Vita

Donald William Millsap was born in 1987 in Kansas City, Kansas to Sandra Jeanne Davidson-Millsap and Donald Scott Millsap. He graduated from Platte City High School in Platte City, Missouri just north of Kansas City, Missouri in May of 2005. He then attended the University of Kansas in Lawrence, Kansas from the fall of 2005 to May 2010 and graduated with two Bachelor of Science degrees in Physics and Astronomy. He was admitted to the graduate program of Nuclear Engineering within the Department of Mechanical Engineering at the University of Texas at Austin in the fall of 2011.

E-mail Address: donwmillsap@gmail.com

This master's thesis was typed by the author.